Journal of Computational and Applied Mathematics 484 (2026) 117448

Contents lists available at ScienceDirect

Journal of Computational and Applied Mathematics

journal homepage: www.elsevier.com/locate/cam

Extended multi-step high-order numerical methods for the nonlinear convection-diffusion-reaction equation with vanishing delay

Qiumei Huang [a], Cheng Wang [b], Gangfan Zhong [a,*]

[a] School of Mathematics, Statistics and Mechanics, Beijing University of Technology, Beijing 100124, China
[b] Department of Mathematics, University of Massachusetts Dartmouth, North Dartmouth, MA 02747, USA

ARTICLE INFO

2000 MSC:
35K55
65M06
65M12

Keywords:
Nonlocal partial differential equation
Nonlinear delay convection-diffusion-reaction equation
Fourth-order long-stencil finite difference approximation
Multi-step scheme
Convergence analysis and error estimate

ABSTRACT

In this paper, we propose two multi-step, linearized numerical schemes for a nonlinear convection-diffusion-reaction (CDR) equation with vanishing delay, a temporally nonlocal partial differential equation. These semi-implicit numerical schemes use a combination of explicit Adams–Bashforth extrapolation for the nonlinear term and implicit Adams–Moulton interpolation for the diffusion term. A long stencil finite difference approximation is employed for the spatial discretization, and a boundary extrapolation is used to prescribe the solution at "ghost" points lying outside of the computational domain. The numerical stability and convergence analysis is provided, and the discrete ℓ^2 convergence estimate is obtained, with fourth-order spatial accuracy and high-order (third- or fourth-order) temporal accuracy. A few numerical experiments are also presented to confirm the theoretical results.

1. Introduction

The partial differential equations incorporating nonlocal effects form a class of problems with broad applications in many scientific areas. For example, a convolution operator stands for a nonlocal spatial effect, and a time-delay composition function represents a temporally nonlocal effect. Some existing works have addressed the numerical approximations for these nonlocal equations [1–4]. In particular, the partial differential equation incorporating a time-delay effect is formulated as

$$U_t + AU = f(U(\boldsymbol{x}, t - \tau(t)), U(\boldsymbol{x}, t)),$$

where A is a linear operator and the delay quantity satisfies $\tau(t) \geq \tau_0 > 0$ or a vanishing one. This equation plays an important role in the simulation of many real-world applications, such as electronic circuits [5], biological systems [6], population problems [7], control theories [8] and so on. Since the 1970s, this kind of equation has been extensively studied, and several important properties such as the existence and stability of the solution have been well understood [9].

It is well known that the solution of most delay partial differential equations (DPDEs) cannot be analytically expressed, which has led to an increasing attention to the numerical study. For example, Wang et al. [10] proposed a posteriori error estimates of Crank–Nicolson–Galerkin type methods for time discretizations of reaction-diffusion equations with time-dependent delay. Tang and

* Corresponding author.
E-mail addresses: qmhuang@bjut.edu.cn (Q. Huang), cwang1@umassd.edu (C. Wang), gfzhong@emails.bjut.edu.cn (G. Zhong).

https://doi.org/10.1016/j.cam.2026.117448
Received 19 September 2025; Received in revised form 9 January 2026
Available online 17 February 2026

Zhang [11,12] constructed fully discrete θ-methods to solve semilinear reaction-diffusion equations with time-dependent delay. Xu and Huang [13] applied a discontinuous Galerkin time stepping method, combined with the standard finite element method in space, to solve semilinear reaction-diffusion equations with constant delay. Dai et al. [14] constructed exponential time differencing-Padé finite element methods for nonlinear convection-diffusion-reaction equations with constant delay. Huang et al. [15] developed exponential Runge–Kutta methods of collocation type for semilinear parabolic problems with time-dependent delay. The numerical research focused on stability analysis for DPDEs with constant delay could be found in [16,17].

DPDEs with time-dependent delay generally provide a more accurate description of the dynamic nature of real-world systems compared to those with constant delay. The existence of the time-dependent delay makes mathematical modeling and numerical solutions more complicated. The delay differential equations (DDEs) and DPDEs with vanishing delay, which is a specific case of time-dependent delay, arise in various phenomena, such as electrodynamics [18], theory of artificial neural networks [19] and many others [20]. At present, there have been quite a few numerical works for solving DDEs with vanishing delay (e.g., [21–23]). On the other hand, for the DPDEs, in which the convection and diffusion processes will play an important role, the numerical study with time-dependent delay (including vanishing type) has been very limited.

In this paper, we consider the following convection-diffusion-reaction (CDR) equation with vanishing delay

$$\partial_t U - \Delta U + \boldsymbol{b}(\boldsymbol{x}) \cdot \nabla U + b_0(\boldsymbol{x}) U = f(U(\theta(t)), U(t)), \qquad (\boldsymbol{x}, t) \in \Omega \times [0, T], \tag{1}$$

$$\frac{\partial U}{\partial \boldsymbol{n}} = 0, \qquad (\boldsymbol{x}, t) \in \partial\Omega \times [0, T], \tag{2}$$

$$u(\boldsymbol{x}, 0) = U_0(\boldsymbol{x}), \qquad \boldsymbol{x} \in \Omega, \tag{3}$$

where the coefficients $\boldsymbol{b}(\boldsymbol{x})$ and $b_0(\boldsymbol{x})$ are C^1 functions on $\overline{\Omega}$. The nonlinear function $f(v_1, v_2) : \mathbb{R}^2 \to \mathbb{R}$ and delay function $\theta(t) : [0, T] \to \mathbb{R}$ are smooth and satisfy

(A1). $\theta(0) = 0$ and $\theta(t) < t$ for $t > 0$; (A2). $\min_{t \in [0,T]} \theta'(t) > 0$.

Regarding the spatial discretization, the fourth-order finite difference method is advantageous as it provides highly accurate numerical solutions and can be efficiently solved using the fast FFT-based method; see the related discussion [24]. In this paper, a fourth-order long-stencil finite difference approximation is employed. In comparison with the fourth-order compact difference approximation involving an additional discrete Poisson-like operator (cf. [25]), the application of the long-stencil fourth-order finite difference approximation could avoid an additional Poisson solver. The fourth-order long-stencil finite difference method has been extensively applied to several kinds of partial differential equations, such as two-dimensional incompressible Boussinesq equation [26,27], three-dimensional geophysical fluid models [28,29], Maxwell's equations [30], Cahn–Hilliard equation [31] and harmonic mapping flow [32], etc.

In the temporal discretization, by combining an explicit Adams–Bashforth extrapolation and a stretched implicit Adams–Moulton method, third- and fourth-order multi-step linearized schemes are proposed for (1). The stability and convergence for such a multi-step, semi-implicit method have been extensively analyzed for many nonlinear PDEs, including viscous Burgers' equation [33], incompressible Navier–Stokes equation [34] and harmonic mapping flow [32]. Unlike standard PDEs, the delayed time value $\theta(t_n)$ in DPDEs may not coincide with the time mesh. Therefore, the delay function $U(\theta(t_n))$ must be approximated using a high-order interpolation approach to maintain overall accuracy consistency. The proposed third-order scheme is a four-step method, requiring numerical approximations for U^n $(n = 1, 2, 3)$ to maintain the convergence rate of $O(\Delta t^3)$. The predictor-corrector method is used to generate the initial data, i.e., a rough approximation is given by the predictor method, and subsequently the accuracy of the approximation in time is enhanced to the third order by several corrections. Such a method could also be applied to the generation of the initial data required for the fourth-order method.

This article is organized as follows. In Section 2, the third-order linearized multi-step scheme is proposed, and the detailed convergence analysis is presented. The fourth-order multi-step linearized scheme is described in Section 3. Some numerical results are presented in Section 4. Finally, some concluding remarks are made in Section 5.

2. The third-order multi-step scheme

In this section, a fully discrete numerical scheme for (1) is constructed via a fourth-order long-stencil finite difference spatial approximation and a third-order multi-step discretization in the temporal direction, and the stability and convergence analysis are provided. For simplicity of presentation, the computational domain is taken as $\Omega = [0, 1]^2$, discretized with a grid size $h = 1/N$, where N denotes the number of numerical mesh cells along each spatial direction. The boundary $\partial\Omega$ is composed of $\Gamma_x : \{y = 0, 1\}$ and $\Gamma_y : \{x = 0, 1\}$.

In this article, $\tilde{D}_x$, $\tilde{D}_y$, D_x^2, D_y^2, D_x^4 and D_y^4 are the standard centered difference operators, to approximate ∂_x, ∂_y, ∂_x^2, ∂_y^2, ∂_x^4 and ∂_y^4, respectively. Subsequently, the standard fourth-order centered long-stencil approximations of ∂_x and ∂_x^2 are given by

$$\begin{aligned}
\mathcal{D}_{x,(4)}^1 w_{i,j} &:= \tilde{D}_x \Big(1 - \frac{h^2}{6} D_x^2\Big) w_{i,j} = \frac{w_{i-2,j} - 8w_{i-1,j} + 8w_{i+1,j} - w_{i+2,j}}{12h} \\
&= \partial_x w(x_i, y_j) + O(h^4), \\
\mathcal{D}_{x,(4)}^2 w_{i,j} &:= \Big(D_x^2 - \frac{h^2}{12} D_x^4\Big) w_{i,j} = \frac{-w_{i-2,j} + 16w_{i-1,j} - 30w_{i,j} + 16w_{i+1,j} - w_{i+2,j}}{12h^2}
\end{aligned}$$

$$= \partial_x^2 w(x_i, y_j) + O(h^4),$$

in which $w_{i,j}$ stands for the point-wise interpolation value of $w(x_i, y_j)$ with $x_i = ih$ and $y_j = jh$. Similar definitions could be applied to $\mathcal{D}^1_{y,(4)}$ and $\mathcal{D}^2_{y,(4)}$. The approximations to the Laplacian operator Δ and the gradient operator ∇ are given by, respectively,

$$\Delta_{h,(4)} := \mathcal{D}^2_{x,(4)} + \mathcal{D}^2_{y,(4)} = \Delta_h - \frac{h^2}{12}(D_x^4 + D_y^4), \tag{4}$$

$$\nabla_{h,(4)} := (\mathcal{D}^1_{x,(4)}, \mathcal{D}^1_{y,(4)})^T, \tag{5}$$

where $\Delta_h = D_x^2 + D_y^2$. In fact, these two operators are $O(h^4)$ approximations to Δ and ∇, respectively, via Taylor expansion.

2.1. Construction of the numerical scheme and the main theoretical result

Let $0 = t_0 < t_1 < \cdots < t_L = T$ be a uniform partition of the time interval with the time step size $\Delta t = T/N_t$ and let $t_n = n\Delta t$ for $n = 0, 1, \dots, N_t$. For the third-order (in time) scheme, the diffusion term is computed by a stretched implicit Adams–Moulton interpolation formula with the time nodes $t_{n+1}, t_{n-1}, t_{n-3}$ involved. The convection term, linear reaction term and nonlinear function are updated by an explicit Adams–Bashforth extrapolation formula, with the time nodes t_n, t_{n-1}, t_{n-2} involved. The delay term $U(\theta(t_n))$ is approximated by an explicit formula. Then the fully discrete scheme is formulated as

$$\begin{aligned}
&\frac{u^{n+1} - u^n}{\Delta t} - \Delta_{h,(4)}\left(\frac{2}{3}u^{n+1} + \frac{5}{12}u^{n-1} - \frac{1}{12}u^{n-3}\right)\\
&= \frac{23}{12}\left(f(\tilde{u}_\theta^n, u^n) - \boldsymbol{b}\cdot\nabla_{h,(4)}u^n - b_0 u^n\right)\\
&\quad - \frac{4}{3}\left(f(\tilde{u}_\theta^{n-1}, u^{n-1}) - \boldsymbol{b}\cdot\nabla_{h,(4)}u^{n-1} - b_0 u^{n-1}\right)\\
&\quad + \frac{5}{12}\left(f(\tilde{u}_\theta^{n-2}, u^{n-2}) - \boldsymbol{b}\cdot\nabla_{h,(4)}u^{n-2} - b_0 u^{n-2}\right),
\end{aligned} \tag{6}$$

for $n \ge 3$, where $u^0 = U_0$. Here, $\tilde{u}_\theta^n := \sum_{i=1}^3 u^{m_n - i} \prod_{j\neq i}^{1\le j\le 3} \frac{\theta(t_n) - t_{m_n - j}}{t_{m_n - i} - t_{m_n - j}}$ is an explicit approximation to $U(\theta(t_n))$, where

$$m_n := \begin{cases} 3, & \text{if } 0 < \theta(t_n) \le 2\Delta t,\\ q, & \text{if } (q-1)\Delta t < \theta(t_n) \le q\Delta t \text{ for some } q > 2. \end{cases}$$

Due to the Neumann boundary condition (2), the value of U on the boundary is not known explicitly, only its normal derivative. Therefore, (6) is applied at every interior computational point (x_i, y_j) for $0 \le i, j \le N$, and some "ghost" point values need to be determined. For brevity of presentation, we concentrate on the boundary section Γ_x with $j = 0$, where $u^{n+1}_{i,-1}$ and $u^{n+1}_{i,-2}$ are needed in the numerical implementation. Local Taylor expansions near the boundary yield

$$\begin{aligned}
U^{n+1}_{i,-1} &= U^{n+1}_{i,1} - 2h\partial_y U^{n+1}_{i,0} - \frac{h^3}{3}\partial_y^3 U^{n+1}_{i,0} + O(h^5),\\
U^{n+1}_{i,-2} &= U^{n+1}_{i,2} - 4h\partial_y U^{n+1}_{i,0} - \frac{8h^3}{3}\partial_y^3 U^{n+1}_{i,0} + O(h^5).
\end{aligned} \tag{7}$$

The homogeneous Neumann boundary condition (2) gives the value of the term $\partial_y U^{n+1}_{i,0}$ in (7). It remains to obtain an approximation to $\partial_y^3 U^{n+1}_{i,0}$ with high-order accuracy. To accomplish this goal, we shall use information from the delay CDR equation. Applying ∂_y to (1) on $t = t_{n+1}$ along Γ_x yields

$$\begin{aligned}
&U^{n+1}_{yt} - (U^{n+1}_{yxx} + U^{n+1}_{yyy}) + \left((b_1)_y U^{n+1}_x + b_1 U^{n+1}_{yx} + (b_2)_y U^{n+1}_y + b_2 U^{n+1}_{yy}\right)\\
&\quad + \left((b_0)_y U^{n+1} + b_0 U^{n+1}_y\right)\\
&= \frac{\partial f}{\partial v_1}(U^{n+1}_\theta, U^{n+1})\cdot (U^{n+1}_\theta)_y + \frac{\partial f}{\partial v_2}(U^{n+1}_\theta, U^{n+1})\cdot U^{n+1}_y, \quad \text{on } \Gamma_x.
\end{aligned} \tag{8}$$

Except for the third, fourth, seventh and eighth terms on the left-hand side of (8), the remaining parts disappear, because of the homogeneous Neumann boundary condition. This in turn reveals that

$$\partial_y^3 U^{n+1}_{i,0} = (\partial_y b_1)_{i,0}\partial_x U^{n+1}_{i,0} + (b_2)_{i,0}\partial_y^2 U^{n+1}_{i,0} + (\partial_y b_0)_{i,0} U^{n+1}_{i,0}. \tag{9}$$

Subsequently, $\partial_y^3 U^{n+1}_{i,0}$ can be approximated by

$$\begin{aligned}
\partial_y^3 U^{n+1}_{i,0} &= (\partial_y b_1)_{i,0}\left(2(2\tilde{D}_x U^n_{i,1} - \tilde{D}_x U^n_{i,2}) - (2\tilde{D}_x U^{n-1}_{i,1} - \tilde{D}_x U^{n-1}_{i,2})\right)\\
&\quad + (b_2)_{i,0}\left(2(2D_y^2 U^n_{i,1} - D_y^2 U^n_{i,2}) - (2D_y^2 U^{n-1}_{i,1} - D_y^2 U^{n-1}_{i,2})\right)\\
&\quad + (\partial_y b_0)_{i,0}(2U^n_{i,0} - U^{n-1}_{i,0}) + O(\Delta t^2 + h^2),
\end{aligned} \tag{10}$$

in which the second-order extrapolations, in both the temporal and spatial directions, have been applied in the derivation. A combination of (7) and (10) gives the boundary extrapolation formulas:

$$\begin{aligned} u_{i,-1}^{n+1} &= u_{i,1}^{n+1} - \frac{h^3}{3}\big((\partial_y b_1)_{i,0}(4\tilde{D}_x u_{i,1}^n - 2\tilde{D}_x u_{i,2}^n - 2\tilde{D}_x u_{i,1}^{n-1} + \tilde{D}_x u_{i,2}^{n-1}) \\ &\quad + (b_2)_{i,0}(4D_y^2 u_{i,1}^n - 2D_y^2 u_{i,2}^n - 2D_y^2 u_{i,1}^{n-1} + D_y^2 u_{i,2}^{n-1}) \\ &\quad + (\partial_y b_0)_{i,0}(2u_{i,0}^n - u_{i,0}^{n-1})\big), \\ u_{i,-2}^{n+1} &= u_{i,2}^{n+1} - \frac{8h^3}{3}\big((\partial_y b_1)_{i,0}(4\tilde{D}_x u_{i,1}^n - 2\tilde{D}_x u_{i,2}^n - 2\tilde{D}_x u_{i,1}^{n-1} + \tilde{D}_x u_{i,2}^{n-1}) \\ &\quad + (b_2)_{i,0}(4D_y^2 u_{i,1}^n - 2D_y^2 u_{i,2}^n - 2D_y^2 u_{i,1}^{n-1} + D_y^2 u_{i,2}^{n-1}) \\ &\quad + (\partial_y b_0)_{i,0}(2u_{i,0}^n - u_{i,0}^{n-1})\big). \end{aligned} \tag{11}$$

The initial values of u^n for $n = 1, 2, 3$ must also be computed to obtain an $O(\Delta t^3)$ temporal error. We employ the predictor-corrector approach to produce the initial data. First, a rough approximation $u_{[1]}^n$ is given by the scheme

$$\frac{u_{[1]}^n - u^{n-1}}{\Delta t} - \Delta_{h,(4)} u_{[1]}^n = f(u^{n-1}, u^{n-1}) - \boldsymbol{b} \cdot \nabla_{h,(4)} u^{n-1} - b_0 u^{n-1}. \tag{12}$$

Here, the term $f(u^{n-1}, u^{n-1})$ is employed as a first-order temporal approximation to $f(U(\theta(t_n)), U(t_n))$, as U^{n-1} is a first-order temporal approximation to both $U(\theta(t_n))$ and $U(t_n)$. Denote $u^{-1} := u_0$ and $t_{-1} := -\Delta t$. Since the resulting $u_{[1]}^n$ only achieves second-order accuracy in time, the temporal accuracy needs to be enhanced by an iterative solver:

$$\begin{aligned} &\frac{u_{[l]}^n - u^{n-1}}{\Delta t} - \Delta_{h,(4)} \frac{u_{[l]}^n + u^{n-1}}{2} \\ &= \frac{1}{2} f\Big(u^{n-1} + \frac{\theta(t_n) - t_{n-1}}{t_n - t_{n-1}}(u_{[l-1]}^n - u^{n-1}), u_{[l-1]}^n\Big) \\ &\quad + \frac{1}{2} f\Big(u^{n-2} + \frac{\theta(t_{n-1}) - t_{n-2}}{t_{n-1} - t_{n-2}}(u^{n-1} - u^{n-2}), u^{n-1}\Big) \\ &\quad - \boldsymbol{b} \cdot \nabla_{h,(4)} \frac{u_{[l-1]}^n + u^{n-1}}{2} - b_0 \frac{u_{[l-1]}^n + u^{n-1}}{2}, \end{aligned} \tag{13}$$

where

$$u^{n-1} + \frac{\theta(t_n) - t_{n-1}}{t_n - t_{n-1}}(u_{[l-1]}^n - u^{n-1}) \quad \text{and} \quad u^{n-2} + \frac{\theta(t_{n-1}) - t_{n-2}}{t_{n-1} - t_{n-2}}(u^{n-1} - u^{n-2})$$

are employed as second-order temporal approximations to the delay terms $U(\theta(t_n))$ and $U(\theta(t_{n-1}))$, respectively. The extrapolation formulas of the ghost points near the boundary $y = 0$ for the scheme (13) are given by

$$\begin{aligned} (u_{[l]}^n)_{i,-1} &= (u_{[l]}^n)_{i,1} - \frac{h^3}{3}\big((\partial_y b_1)_{i,0}(2\tilde{D}_x(u^{n-1})_{i,1} - \tilde{D}_x(u^{n-1})_{i,2}) \\ &\quad + (\partial_y b_0)_{i,0}(u^{n-1})_{i,0} + (b_2)_{i,0}(2D_y^2(u^{n-1})_{i,1} - D_y^2(u^{n-1})_{i,2})\big), \\ (u_{[l]}^n)_{i,-2} &= (u_{[l]}^n)_{i,2} - \frac{8h^3}{3}\big((\partial_y b_1)_{i,0}(2\tilde{D}_x(u^{n-1})_{i,1} - \tilde{D}_x(u^{n-1})_{i,2}) \\ &\quad + (\partial_y b_0)_{i,0}(u^{n-1})_{i,0} + (b_2)_{i,0}(2D_y^2(u^{n-1})_{i,1} - D_y^2(u^{n-1})_{i,2})\big). \end{aligned}$$

The corresponding formulas of one-sided extrapolation of ghost points around the other three boundaries can be performed in a similar way. We skip it for the sake of brevity. Taking $u^i = u_{[3]}^i$ for $i = 1, 2, 3$, it could be proved that the third-order numerical accuracy (in time) is reached for these initial values.

To carry out the convergence analysis, we need to introduce the following discrete ℓ^2 inner product in 2D space:

$$\begin{aligned} &\langle w, v \rangle = h\Big(\frac{1}{2}\langle w_{x_0}, v_{x_0}\rangle_y + \sum_{i=1}^{N-1}\langle w_{x_i}, v_{x_i}\rangle_y + \frac{1}{2}\langle w_{x_N}, v_{x_N}\rangle_y\Big), \\ &\quad \text{where } \langle w_{x_{i_1}}, v_{x_{i_2}}\rangle_y = h\Big(\frac{1}{2} w_{i_1,0} v_{i_2,0} + \sum_{j=1}^{N-1} w_{i_1,j} v_{i_2,j} + \frac{1}{2} w_{i_1,N} v_{i_2,N}\Big). \end{aligned}$$

The corresponding discrete ℓ^2 norm $\|\cdot\|_2$ can be similarly defined. In addition, the discrete ℓ^2 norm for the discrete gradient turns out to be

$$\begin{aligned} &\|\nabla_h w\|_2^2 = \|D_x w\|_2^2 + \|D_y w\|_2^2, \quad \text{with} \\ &\|D_x w\|_2^2 = h\sum_{i=0}^{N-1}\langle D_x^+ w_{x_i}, D_x^+ w_{x_i}\rangle_y, \quad \text{where } D_x^+ w_{i,j} = \frac{w_{i+1,j} - w_{i,j}}{h}, \end{aligned}$$

$$\|D_y w\|_2^2 = h\sum_{j=0}^{N-1}\langle D_y^+ w_{y_j}, D_y^+ w_{y_j}\rangle_x, \quad \text{where } D_y^+ w_{i,j} = \frac{w_{i,j+1}-w_{i,j}}{h}.$$

We denote $\bar{w}$ as the even-symmetric extension of w, that is $\bar{w}_{i,j} = w_{i,j}$ and $\bar{w}_{i,-2} = w_{i,2}$, $\bar{w}_{i,-1} = w_{i,1}$, $\bar{w}_{-2,j} = w_{2,j}$, $\bar{w}_{-1,j} = w_{1,j}$ for any $0 \le i,j \le N$. Notice that $\langle D_x^2\bar{w}, \bar{w}\rangle = -\|D_x\bar{w}\|_2^2$ and $\langle D_x^4\bar{w}, \bar{w}\rangle = \|D_x^2\bar{w}\|_2^2$. This is the crucial reason for the choice of even-symmetric extrapolation for u^n on the boundary. For convenience, we introduce the following norm

$$\|D_x^2 w\|_{2,n}^2 = \|D_x^2\bar{w}\|_2^2, \quad \|D_y^2 w\|_{2,n}^2 = \|D_y^2\bar{w}\|_2^2.$$

In addition, the discrete ℓ^∞ norm, defined by $\|w\|_\infty = \max_{i,j}|w_{i,j}|$ for any grid function w, is needed in the later analysis.

We denote by U the exact solution of the delay CDR equation (1)–(3), and extend U smoothly to $[-\delta, 1+\delta]^2$. In the later sections, it is assumed that $\|\boldsymbol{b}\|_{C^1} + \|b_0\|_{C^1} \le \mathcal{M}$ and $\|U\|_{W^{3,\infty}(0,T;C^{7,\alpha}(\overline{\Omega}))} \le C^*$, where $C^{7,\alpha}(\overline{\Omega})$ consists of functions that are continuously differentiable up to order 7 in $\overline{\Omega}$, with the 7th-order derivatives being Hölder continuous with exponent α (cf. [35]). The point-wise numerical error grid function is defined as

$$e^k := U^k - u^k, \quad k = 0, 1, \dots, N_t.$$

The convergence result is stated below.

Theorem 1. *Assume that $f = f(v_1, v_2) \in C^3(\mathbb{R}^2)$ and $\theta \in C^3[0,T]$. Let $U \in W^{3,\infty}(0,T;C^{7,\alpha}(\overline{\Omega}))$ be the exact solution of the delay CDR equation (1)–(3), and u^n be the fully discrete numerical solution obtained by (6). As $\Delta t, h \to 0$ under a linear refinement requirement $\Delta t \le \tilde{C}h$, we obtain the following result: for $n = 1, 2, \dots, N_t$,*

$$\|u^n - U^n\|_2 \le C(\Delta t^3 + h^4), \quad \textit{with } C \textit{ independent of } \Delta t \textit{ and } h.$$

2.2. *Proof of Theorem 1: Convergence analysis for the third-order multi-step scheme (6)*

The procedure of the convergence proof is standard, composed of the consistency analysis and error estimate. We begin with the consistency analysis in Section 2.2.1. Before analyzing the ℓ^2 error estimate (in Section 2.2.3), we make an a-priori ℓ^∞ assumption (in Section 2.2.2) for the numerical error function, which provides a foundation for the inner product estimates involving nonlinear and convection terms. Finally, the proof is completed by recovering the a-priori ℓ^∞ bound in Section 2.2.4.

2.2.1. *Consistency analysis*

The consistency analysis of scheme (6) for $n \ge 3$ is given in this subsection. Denote $\tilde{U}_\theta^n := \sum_{i=1}^3 U^{m_n-i}\prod_{j\ne i}^{1\le j\le 3}\frac{\theta(t_n)-t_{m_n-j}}{t_{m_n-i}-t_{m_n-j}}$ as the approximation to $U_\theta(t) := U(\theta(t))$. Taylor expansion in time indicates the following truncation error estimates:

$$U^{n+1} - U^n = \int_{t_n}^{t_{n+1}} \partial_t U(t)dt,$$

$$\Delta\left(\frac{2}{3}U^{n+1} + \frac{5}{12}U^{n-1} - \frac{1}{12}U^{n-3}\right) = \frac{1}{\Delta t}\int_{t_n}^{t_{n+1}} \Delta U(t)dt + \tau_1^{n+1},$$

$$\text{with } \sum_{n=4}^{N}\|\tau_1^n\|_\infty \le C\Delta t^3\|U\|_{H^3(0,T;C^2)} \le C\Delta t^3,$$

$$\frac{23}{12}\left(f(U_\theta^n, U^n) - \boldsymbol{b}\cdot\nabla U^n - b_0U^n\right) - \frac{4}{3}\left(f(U_\theta^{n-1}, U^{n-1}) - \boldsymbol{b}\cdot\nabla u^{n-1} - b_0U^n\right)$$
$$+ \frac{5}{12}\left(f(U_\theta^{n-2}, U^{n-2}) - \boldsymbol{b}\cdot\nabla U^{n-2} - b_0U^{n-2}\right)$$
$$= \frac{1}{\Delta t}\int_{t_n}^{t_{n+1}}\left(f(U(\theta(t)), U(t)) - \boldsymbol{b}\cdot\nabla U(t) - b_0U(t)\right)dt + \tau_2^{n+1},$$

$$\text{with } \sum_{n=4}^{N}\|\tau_2^n\|_\infty \le C\Delta t^3(\|f(U_\theta, U)\|_{H^3(0,T;L^\infty)} + \|U\|_{H^3(0,T;C^1)}) \le C\Delta t^3,$$

$$\frac{23}{12}f(\tilde{U}_\theta^n, U^n) - \frac{4}{3}f(\tilde{U}_\theta^{n-1}, U^{n-1}) + \frac{5}{12}f(\tilde{U}_\theta^{n-2}, U^{n-2})$$
$$= \frac{23}{12}f(U_\theta^n, U^n) - \frac{4}{3}f(U_\theta^{n-1}, U^{n-1}) + \frac{5}{12}f(U_\theta^{n-2}, U^{n-2}) + \tau_3^{n+1},$$

$$\text{with } \sum_{n=4}^{N}\|\tau_3^n\|_\infty \le C\Delta t^3\|U\|_{H^3(0,T;L^\infty)} \le C\Delta t^3.$$

Consequently, a combination of the above estimates implies the third-order temporal consistency of the exact solution U:

$$\begin{aligned}&\frac{U^{n+1}-U^n}{\Delta t}-\Delta\Big(\frac{2}{3}U^{n+1}+\frac{5}{12}U^{n-1}-\frac{1}{12}U^{n-3}\Big)\\&=\frac{23}{12}\Big(f(\tilde U_\theta^n,U^n)-\boldsymbol{b}\cdot\nabla U^n-b_0U^n\Big)\\&\quad-\frac{4}{3}\Big(f(\tilde U_\theta^{n-1},U^{n-1})-\boldsymbol{b}\cdot\nabla U^{n-1}-b_0U^{n-1}\Big)\\&\quad+\frac{5}{12}\Big(f(\tilde U_\theta^{n-2},U^{n-2})-\boldsymbol{b}\cdot\nabla U^{n-2}-b_0U^{n-2}\Big)+\tau_4^{n+1},\end{aligned}\tag{14}$$

with $\sum_{n=4}^N\|\tau_4^n\|_\infty\le C\Delta t^3$. A combination of (14) and (4)–(5) yields the desired consistency estimate for the fully discrete scheme (6), with third-order temporal accuracy and fourth-order spatial accuracy:

$$\begin{aligned}&\frac{U^{n+1}-U^n}{\Delta t}-\Delta_{h,(4)}\Big(\frac{2}{3}U^{n+1}+\frac{5}{12}U^{n-1}-\frac{1}{12}U^{n-3}\Big)\\&=\frac{23}{12}\Big(f(\tilde U_\theta^n,U^n)-\boldsymbol{b}\cdot\nabla_{h,(4)}U^n-b_0U^n\Big)\\&\quad-\frac{4}{3}\Big(f(\tilde U_\theta^{n-1},U^{n-1})-\boldsymbol{b}\cdot\nabla_{h,(4)}U^{n-1}-b_0U^{n-1}\Big)\\&\quad+\frac{5}{12}\Big(f(\tilde U_\theta^{n-2},U^{n-2})-\boldsymbol{b}\cdot\nabla_{h,(4)}U^{n-2}-b_0U^{n-2}\Big)+\tau^{n+1},\end{aligned}\tag{15}$$

with $\sum_{n=4}^N\|\tau^n\|_\infty\le C(\Delta t^3+h^4)$. In turn, subtracting the numerical scheme (6) from the consistency estimate (15) gives

$$\begin{aligned}&\frac{e^{n+1}-e^n}{\Delta t}-\Delta_{h,(4)}\Big(\frac{2}{3}e^{n+1}+\frac{5}{12}e^{n-1}-\frac{1}{12}e^{n-3}\Big)\\&=\frac{23}{12}(\mathcal{NLE}^n-\boldsymbol{b}\cdot\nabla_{h,(4)}e^n-b_0e^n)-\frac{4}{3}(\mathcal{NLE}^{n-1}-\boldsymbol{b}\cdot\nabla_{h,(4)}e^{n-1}-b_0e^{n-1})\\&\quad+\frac{5}{12}(\mathcal{NLE}^{n-2}-\boldsymbol{b}\cdot\nabla_{h,(4)}e^{n-2}-b_0e^{n-2})+\tau^{n+1},\end{aligned}\tag{16}$$

where $\mathcal{NLE}^k=f(\tilde U_\theta^k,U^k)-f(\tilde u_\theta^k,u^k)$ for $k=n-2,n-1,n$.

2.2.2. An a-priori ℓ^∞ assumption

To deal with the multi-step method (6), we assume a-priori that the numerical error function has an ℓ^∞ bound at the previous time steps:

$$\|e^k\|_\infty\le h^{\frac{3}{2}}\quad\text{for } k=0,1,2,\dots,n.\tag{17}$$

In particular, such an a-priori assumption is also satisfied at the initial steps $k=0,1,2,3$. In fact, an application of the inverse inequality to the ℓ^2 error estimate (A.10) implies that

$$\|e^k\|_\infty\ \le 2h^{-1}\|e^k\|_2\le 2C_0^{\frac{1}{2}}h^{-1}(\Delta t^3+h^4)\le 2\,C_0^{\frac{1}{2}}(\tilde C^3h^2+h^3)\le h^{\frac{3}{2}},\ \ k=0,1,2,3.$$

Subsequently, under the a-priori assumption (17), the ℓ^∞ bound of the numerical solution at these time steps could be derived as

$$\|u^k\|_\infty=\|U^k-e^k\|_\infty\le\|U^k\|_\infty+\|e^k\|_\infty\le C^*+1,\ \ k=0,1,2,\dots,n.$$

2.2.3. ℓ^2 error analysis

Taking the discrete ℓ^2 inner product of (16) with $2\Delta te^{n+1}$ yields

$$\begin{aligned}&\langle e^{n+1}-e^n,2e^{n+1}\rangle-\Delta t\Big\langle\Delta_{h,(4)}\big(\frac{4}{3}e^{n+1}+\frac{5}{6}e^{n-1}-\frac{1}{6}e^{n-3}\big),e^{n+1}\Big\rangle\\&=\frac{23}{6}\Delta t\langle\mathcal{NLE}^n-\boldsymbol{b}\cdot\nabla_{h,(4)}e^n-b_0e^n,e^{n+1}\rangle\\&\quad-\frac{8}{3}\Delta t\langle\mathcal{NLE}^{n-1}-\boldsymbol{b}\cdot\nabla_{h,(4)}e^{n-1}-b_0e^{n-1},e^{n+1}\rangle\\&\quad+\frac{5}{6}\Delta t\langle\mathcal{NLE}^{n-2}-\boldsymbol{b}\cdot\nabla_{h,(4)}e^{n-2}-b_0e^{n-2},e^{n+1}\rangle+2\Delta t\langle\tau^{n+1},e^{n+1}\rangle.\end{aligned}\tag{18}$$

The Cauchy inequality could be used to bound the time marching, truncation error and linear reaction error terms:

$$\langle e^{n+1}-e^n,2e^{n+1}\rangle=\|e^{n+1}\|_2^2-\|e^n\|_2^2+\|e^{n+1}-e^n\|_2^2,\tag{19}$$

$$2\langle\tau^{n+1},e^{n+1}\rangle\le\|\tau^{n+1}\|_2^2+\|e^{n+1}\|_2^2,\tag{20}$$

$$\begin{aligned}&-\frac{23}{6}\langle b_0e^n,e^{n+1}\rangle+\frac{8}{3}\langle b_0e^{n-1},e^{n+1}\rangle-\frac{5}{6}\langle b_0e^{n-2},e^{n+1}\rangle\\&\qquad\le C_1(3\|e^{n+1}\|_2^2+\|e^n\|_2^2+\|e^{n-1}\|_2^2+\|e^{n-2}\|_2^2),\ \ C_1:=\frac{23}{12}\mathcal{M}.\end{aligned}\tag{21}$$

For the nonlinear error parts, we focus on the term $\mathcal{NLE}^n$, and the two other ones could be similarly treated. An application of the mean value theorem implies that

$$\begin{aligned}\|\mathcal{NLE}^n\|_2 &\le \|f(\tilde{U}_\theta^n, U^n) - f(\tilde{U}_\theta^n, u^n)\|_2 + \|f(\tilde{U}_\theta^n, u^n) - f(\tilde{u}_\theta^n, u^n)\|_2 \\ &\le \max_{0\le s\le 1}\left\|\frac{\partial f}{\partial v_1}(\tilde{U}_\theta^n, U^n + s(u^n - U^n))\right\|_\infty \cdot \|U^n - u^n\|_2 \\ &\quad + \max_{0\le s\le 1}\left\|\frac{\partial f}{\partial v_2}(\tilde{U}_\theta^n + s(\tilde{u}_\theta^n - \tilde{U}_\theta^n), u^n)\right\|_\infty \cdot \|\tilde{u}_\theta^n - \tilde{U}_\theta^n\|_2. \end{aligned} \tag{22}$$

Recalling that $\|U^k\|_\infty \le C^*$ and $\|u^k\|_\infty \le C^* + 1$ for $k = 0, 1, \dots, n$, we obtain

$$\begin{aligned}&\|\tilde{u}_\theta^n\|_\infty \le 9(\|u^{m_n-1}\|_\infty + \|u^{m_n-2}\|_\infty + \|u^{m_n-3}\|_\infty) \le 27(C^*+1),\\ &\|\tilde{U}_\theta^n\|_\infty \le 9(\|U^{m_n-1}\|_\infty + \|U^{m_n-2}\|_\infty + \|U^{m_n-3}\|_\infty) \le 27C^*,\\ &\|U^n + s(u^n - U^n)\|_\infty \le \|U^n\|_\infty + \|u^n\|_\infty \le 2C^* + 1,\\ &\|\tilde{U}_\theta^n + s(\tilde{u}_\theta^n - \tilde{U}_\theta^n)\|_\infty \le \|\tilde{U}_\theta^n\|_\infty + \|\tilde{u}_\theta^n\|_\infty \le 27(2C^*+1) =: K.\end{aligned}$$

Combining this with (22) yields

$$\begin{aligned}\|\mathcal{NLE}^n\|_2 &\le \max_{|\boldsymbol{\alpha}|=1, |v_1|, |v_2| \le K} |\partial^{\boldsymbol{\alpha}} f(v_1, v_2)| \big(\|e^n\|_2 + 9(\|e^{m_n-1}\|_2 + \|e^{m_n-2}\|_2 + \|e^{m_n-3}\|_2)\big) \\ &\le C_2(\|e^n\|_2 + \|e^{m_n-1}\|_2 + \|e^{m_n-2}\|_2 + \|e^{m_n-3}\|_2),\end{aligned} \tag{23}$$

with $C_2 := 9 \cdot \max_{|\boldsymbol{\alpha}|=1, |v_1|, |v_2| \le K} |\partial^{\boldsymbol{\alpha}} f(v_1, v_2)|$. By using Cauchy's inequality and (23), we see that

$$\frac{23}{6}|\langle \mathcal{NLE}^n, e^{n+1}\rangle| \le C_3\|e^{n+1}\|_2^2 + C_2^2\|e^n\|_2^2 + C_2^2\sum_{k=1}^{3}\|e^{m_n-k}\|_2^2, \tag{24}$$

with $C_3 := (\frac{23}{6})^2$. Similar estimates could be derived for the other two nonlinear parts

$$\frac{8}{3}|\langle \mathcal{NLE}^{n-1}, e^{n+1}\rangle| \le C_3\|e^{n+1}\|_2^2 + C_2^2(\|e^{n-1}\|_2^2 + \sum_{k=1}^{3}\|e^{m_{n-1}-k}\|_2^2), \tag{25}$$

$$\frac{5}{6}|\langle \mathcal{NLE}^{n-2}, e^{n+1}\rangle| \le C_3\|e^{n+1}\|_2^2 + C_2^2(\|e^{n-2}\|_2^2 + \sum_{k=1}^{3}\|e^{m_{n-2}-k}\|_2^2). \tag{26}$$

Regarding the estimate of the diffusion error term, a typical theoretical difficulty arises if a direct truncation error estimate is performed, due to the loss of accuracy near the boundary by a formal observation. To derive a full accuracy estimate, an approximation of the exact solution U^{n+1} has to be constructed by adding an $O(h^4)$ term to U^{n+1} to satisfy the truncation error fully to fourth order:

$$\mathcal{U}^{n+1} := U^{n+1} + h^4\hat{U}^{n+1}, \quad n \ge 3,$$

where the correction function $\hat{U}^{n+1}$ satisfies the Poisson equation

$$\Delta\hat{U}^{n+1} = \mathcal{K}^{n+1} \tag{27}$$

with the prescribed Neumann boundary conditions (by setting $\kappa := \Delta t/h$)

$$\begin{aligned}\partial_y\hat{U}^{n+1}(x,0) &= -\frac{1}{12}(\beta^{n+1}(x,0) + \kappa^2\gamma^{n+1}(x,0)) + \frac{1}{80}\partial_y^5 U^{n+1}(x,0),\\ \partial_y\hat{U}^{n+1}(x,1) &= -\frac{1}{12}(\beta^{n+1}(x,1) + \kappa^2\gamma^{n+1}(x,1)) + \frac{1}{80}\partial_y^5 U^{n+1}(x,1),\\ \partial_x\hat{U}^{n+1}(0,y) &= -\frac{1}{12}(\beta^{n+1}(0,y) + \kappa^2\gamma^{n+1}(0,y)) + \frac{1}{80}\partial_x^5 U^{n+1}(0,y),\\ \partial_x\hat{U}^{n+1}(1,y) &= -\frac{1}{12}(\beta^{n+1}(1,y) + \kappa^2\gamma^{n+1}(1,y)) + \frac{1}{80}\partial_x^5 U^{n+1}(1,y).\end{aligned} \tag{28}$$

The functions β^{n+1} and γ^{n+1} on the boundary section Γ_x with $y = 0$ are given by

$$\begin{aligned}\beta^{n+1} &:= (\partial_y b_1)\cdot\left(\partial_y^2\partial_x U^{n+1} - \frac{h^2}{6}\partial_x^3 U^{n+1}\right) + b_2\cdot\left(\frac{11}{12}\partial_y^4 U^{n+1}\right),\\ \gamma^{n+1} &:= (\partial_y b_1)\cdot(\partial_t^2\partial_x U^{n+1}) + b_2\cdot(\partial_t^2\partial_y^2 U^{n+1}) + (\partial_y b_0)\cdot(\partial_t^2 U^{n+1}).\end{aligned}$$

As we shall see in (31), this construction groups the second-order remainder terms. The formulas on the other three boundaries can be given in a similar way. The scalar quantity $\mathcal{K}^{n+1}$ is chosen as $\mathcal{K}^{n+1} = \frac{1}{|\Omega|}\int_{\partial\Omega}\frac{\partial\hat{U}^{n+1}}{\partial\boldsymbol{n}}d\boldsymbol{n}$ to maintain a consistency with the Neumann boundary condition. An application of the Schauder estimate to the Poisson equation (27) implies that

$$\|\hat{U}^{n+1}\|_{C^{m,\alpha}} \le C\|U^{n+1}\|_{W^{2,\infty}(0,T;C^{m+4,\alpha})}, \quad \text{for } m \ge 2. \tag{29}$$

In turn, local Taylor expansions for the exact solution U^{n+1} reveal that

$$\begin{aligned} U_{i,-1}^{n+1} &= U_{i,1}^{n+1} - \frac{h^3}{3}\partial_y^3 U_{i,0}^{n+1} - \frac{h^5}{60}\partial_y^5 U_{i,0}^{n+1} + O(h^7)\|U^{n+1}\|_{C^7}, \\ U_{i,-2}^{n+1} &= U_{i,2}^{n+1} - \frac{8h^3}{3}\partial_y^3 U_{i,0}^{n+1} - \frac{32h^5}{60}\partial_y^5 U_{i,0}^{n+1} + O(h^7)\|U^{n+1}\|_{C^7}. \end{aligned} \tag{30}$$

Recalling the derivation for $\partial_y^3 U_{i,0}^{n+1}$ in (9) and using the Taylor expansions

$$\begin{aligned} &2(2\tilde{D}_x U_{i,1}^n - \tilde{D}_x U_{i,2}^n) - (2\tilde{D}_x U_{i,1}^{n-1} - \tilde{D}_x U_{i,2}^{n-1}) \\ &\quad = \partial_x U_{i,0}^{n+1} - \Delta t^2 \partial_t^2 \partial_x U_{i,0}^{n+1} - h^2 \partial_y^2 \partial_x U_{i,0}^{n+1} + \frac{h^2}{6}\partial_x^3 U_{i,0}^{n+1} \\ &\qquad + O(\Delta t^3 + h^3)\|U\|_{W^{3,\infty}(0,T;C^4)}, \\ &2(2D_y^2 U_{i,1}^n - D_y^2 U_{i,2}^n) - (2D_y^2 U_{i,1}^{n-1} - D_y^2 U_{i,2}^{n-1}) \\ &\quad = \partial_y^2 U_{i,0}^{n+1} - \Delta t^2 \partial_t^2 \partial_y^2 U_{i,0}^{n+1} - \frac{11h^2}{12}\partial_y^4 U_{i,0}^{n+1} + O(\Delta t^3 + h^3)\|U\|_{W^{3,\infty}(0,T;C^5)}, \\ &2U_{i,0}^n - U_{i,0}^{n-1} = U_{i,0}^{n+1} - \Delta t^2 \partial_t^2 U_{i,0}^{n+1} + O(\Delta t^3)\|U\|_{W^{3,\infty}(0,T;C^0)}, \end{aligned}$$

we arrive at

$$\begin{aligned} \partial_y^3 U_{i,0}^{n+1} = &(\partial_y b_1)_{i,0}(4\tilde{D}_x U_{i,1}^n - 2\tilde{D}_x U_{i,2}^n - 2\tilde{D}_x U_{i,1}^{n-1} + \tilde{D}_x U_{i,2}^{n-1}) \\ &+ (b_2)_{i,0}(4D_y^2 U_{i,1}^n - 2D_y^2 U_{i,2}^n - 2D_y^2 U_{i,1}^{n-1} + D_y^2 U_{i,2}^{n-1}) \\ &+ (\partial_y b_0)_{i,0}(2U_{i,0}^n - U_{i,0}^{n-1}) + h^2 \beta_{i,0}^{n+1} + \Delta t^2 \gamma_{i,0}^{n+1} \\ &+ O(\Delta t^3 + h^3)\|U\|_{W^{3,\infty}(0,T;C^5)}. \end{aligned} \tag{31}$$

A substitution of the boundary condition (28) into the Taylor expansions of $\hat{U}^{n+1}$, along with the fact that $\|\hat{U}^{n+1}\|_{C^3} \le C\|U\|_{W^{2,\infty}(0,T;C^{7,\alpha})}$ (by (29)), leads to

$$\begin{aligned} \hat{U}_{i,-1}^{n+1} &= \hat{U}_{i,1}^{n+1} - 2h\partial_y \hat{U}_{i,0}^{n+1} + O(h^3)\partial_y^3 \hat{U}_{i,0}^{n+1} \\ &= \hat{U}_{i,1}^{n+1} + \frac{h}{6}(\beta_{i,0}^{n+1} + \kappa^2 \gamma_{i,0}^{n+1}) - \frac{h}{40}\partial_y^5 U_{i,0}^{n+1} + O(h^3)\|U\|_{W^{2,\infty}(0,T;C^{7,\alpha})}, \\ \hat{U}_{i,-2}^{n+1} &= \hat{U}_{i,2}^{n+1} - 4h\partial_y \hat{U}_{i,0}^{n+1} + O(h^3)\partial_y^3 \hat{U}_{i,0}^{n+1}, \\ &= \hat{U}_{i,2}^{n+1} + \frac{h}{3}(\beta_{i,0}^{n+1} + \kappa^2 \gamma_{i,0}^{n+1}) - \frac{h}{20}\partial_y^5 U_{i,0}^{n+1} + O(h^3)\|U\|_{W^{2,\infty}(0,T;C^{7,\alpha})}. \end{aligned} \tag{32}$$

A combination of (30)–(32) results in the following estimates for $\mathcal{U}^{n+1}$:

$$\begin{aligned} \mathcal{U}_{i,-1}^{n+1} = \mathcal{U}_{i,1}^{n+1} - \frac{h^3}{3}\big(&(\partial_y b_1)_{i,0}(4\tilde{D}_x U_{i,1}^n - 2\tilde{D}_x U_{i,2}^n - 2\tilde{D}_x U_{i,1}^{n-1} + \tilde{D}_x U_{i,2}^{n-1}) \\ &+ (b_2)_{i,0}(4D_y^2 U_{i,1}^n - 2D_y^2 U_{i,2}^n - 2D_y^2 U_{i,1}^{n-1} + D_y^2 U_{i,2}^{n-1}) \\ &+ (\partial_y b_0)_{i,0}(2U_{i,0}^n - U_{i,0}^{n-1})\big) - \frac{h^5}{6}(\beta_{i,0}^{n+1} + \kappa^2 \gamma_{i,0}^{n+1}) - \frac{h^5}{24}\partial_y^5 U_{i,0}^{n+1} \\ &+ O(h^6)\|U\|_{W^{3,\infty}(0,T;C^{7,\alpha})}, \\ \mathcal{U}_{i,-2}^{n+1} = \mathcal{U}_{i,2}^{n+1} - \frac{8h^3}{3}\big(&(\partial_y b_1)_{i,0}(4\tilde{D}_x U_{i,1}^n - 2\tilde{D}_x U_{i,2}^n - 2\tilde{D}_x U_{i,1}^{n-1} + \tilde{D}_x U_{i,2}^{n-1}) \\ &+ (b_2)_{i,0}(4D_y^2 U_{i,1}^n - 2D_y^2 U_{i,2}^n - 2D_y^2 U_{i,1}^{n-1} + D_y^2 U_{i,2}^{n-1}) \\ &+ (\partial_y b_0)_{i,0}(2U_{i,0}^n - U_{i,0}^{n-1})\big) - \frac{7h^5}{3}(\beta_{i,0}^{n+1} + \kappa^2 \gamma_{i,0}^{n+1}) - \frac{7h^5}{12}\partial_y^5 U_{i,0}^{n+1} \\ &+ O(h^6)\|U\|_{W^{3,\infty}(0,T;C^{7,\alpha})}. \end{aligned} \tag{33}$$

Similar results can be derived on the other three boundary segments, namely $y = 1$, $x = 0$ and $x = 1$.

A direct consequence of the Schauder estimate (29) is observed:

$$\|\hat{U}^{n+1}\|_{W_h^{2,\infty}} \le C\|\hat{U}^{n+1}\|_{C^{2,\alpha}} \le C\|U\|_{W^{2,\infty}(0,T;C^{6,\alpha})}, \tag{34}$$

in which $\|\cdot\|_{W_h^{m,\infty}}$ represents the maximum value, at grids points, of the given function up to mth finite-difference, over the domain Ω. Subsequently, we get

$$\|\mathcal{U}^{n+1} - U^{n+1}\|_{W_h^{2,\infty}} = h^4\|\hat{U}^{n+1}\|_{W_h^{2,\infty}} \le Ch^4\|U\|_{W^{2,\infty}(0,T;C^{6,\alpha})}.$$

Denote $\hat{e}^{n+1} := \mathcal{U}^{n+1} - u^{n+1}$. Subtracting (11) from (33) gives

$$\begin{aligned} \hat{e}^{n+1}_{i,-1} &= \hat{e}^{n+1}_{i,1} + \frac{h^3}{3} q^{n+1}_{i,0} - \frac{h^5}{6} p^{n+1}_{i,0} - \frac{h^5}{24} r^{n+1}_{i,0} + \xi^{n+1}_{i,0}, \\ \hat{e}^{n+1}_{i,-2} &= \hat{e}^{n+1}_{i,2} + \frac{8h^3}{3} q^{n+1}_{i,0} - \frac{7h^5}{3} p^{n+1}_{i,0} - \frac{7h^5}{12} r^{n+1}_{i,0} + \zeta^{n+1}_{i,0}, \end{aligned} \tag{35}$$

with

$$\begin{aligned} q^{n+1}_{i,0} &= -(\partial_y b_1)_{i,0}(4\tilde{D}_x e^n_{i,1} - 2\tilde{D}_x e^{n-1}_{i,2} - 2\tilde{D}_x e^{n-1}_{i,1} + \tilde{D}_x e^{n-1}_{i,2}) \\ &\quad - (b_2)_{i,0}(4D_y^2 e^n_{i,1} - 2D_y^2 e^n_{i,2} - 2D_y^2 e^{n-1}_{i,1} + D_y^2 e^{n-1}_{i,2}) \\ &\quad - (\partial_y b_0)_{i,0}(2e^n_{i,0} - e^{n-1}_{i,0}), \\ p^{n+1}_{i,0} &= \beta^{n+1}_{i,0} + \kappa^2 \gamma^{n+1}_{i,0}, \quad r^{n+1}_i = \partial_y^5 U^{n+1}_{i,0}, \\ |\xi^{n+1}_{i,0}|, |\zeta^{n+1}_{i,0}| &\le C h^6 \|U\|_{W^{3,\infty}(0,T;C^{7,\alpha})}. \end{aligned} \tag{36}$$

Similar results can be obtained on the other three boundary segments. Notice that the $O(h^5)$ coefficients of $\hat{e}^{n+1}_{i,-1}$ and $\hat{e}^{n+1}_{i,-2}$ have the ratio $1:14$, and such a ratio is needed for the error analysis in terms of the diffusion term. This fact turns out to be the reason for the choice of the boundary condition for $\hat{U}^{n+1}$ in (28).

The diffusion estimate is stated in the next two propositions. For convenience, we denote $e^n, \hat{e}^n := 0$ for $n \le 0$.

Proposition 1. *The following inequality is valid for $n \ge 3$:*

$$\begin{aligned} &- \langle \big(\Delta_h - \frac{h^2}{12}(D_x^4 + D_y^4)\big) e^{n+1}, e^{n+1} \rangle \\ &\ge \frac{45}{48}\|\nabla_h e^{n+1}\|_2^2 + \frac{46h^2}{576}(\|D_x^2 e^{n+1}\|_{2,n}^2 + \|D_y^2 e^{n+1}\|_{2,n}^2) - C_{22}h^8 \\ &\quad - \frac{h^2}{576}\sum_{k=0}^{1}(\|D_x^2 e^{n-k}\|_{2,n}^2 + \|D_y^2 e^{n-k}\|_{2,n}^2) - C_{22}\sum_{k=-1}^{3}\|e^{n-k}\|_2^2 \\ &\quad - C_{22}h^2\sum_{k=0}^{3}\|\nabla_h e^{n-k}\|_2^2 - C_{22}h^3\sum_{k=0}^{3}(\|D_x^2 e^{n-k}\|_{2,n}^2 + \|D_y^2 e^{n-k}\|_{2,n}^2). \end{aligned} \tag{37}$$

Proof. A lower bound for $-\langle \hat{e}^{n+1}, (\Delta_h - \frac{h^2}{12}(D_x^4 + D_y^4))\hat{e}^{n+1}\rangle$ is derived, and the desired estimate (37) is obtained by using (34). Based on the boundary extrapolation (35), an application of the summation-by-parts formula indicates that

$$\begin{aligned} &\langle \big(\Delta_h - \frac{h^2}{12}(D_x^4 + D_y^4)\big)\hat{e}^{n+1}, \hat{e}^{n+1} \rangle \\ &= -\|\nabla_h \hat{e}^{n+1}\|_2^2 - \frac{h^2}{12}(\|D_x^2 \hat{e}^{n+1}\|_{2,n}^2 - \|D_y^2 \hat{e}^{n+1}\|_{2,n}^2) + \mathcal{B} \\ &\le -\frac{47}{48}\|\nabla_h e^{n+1}\|_2^2 - \frac{47h^2}{576}(\|D_x^2 e^{n+1}\|_{2,n}^2 - \|D_y^2 e^{n+1}\|_{2,n}^2) + \mathcal{B} + C_4 h^8, \end{aligned} \tag{38}$$

in which (34) has been used in the last inequality. The boundary term is decomposed as $\mathcal{B} = \mathcal{B}^1 + \mathcal{B}^2 + \mathcal{B}^3 + \mathcal{B}^4$, in which $\mathcal{B}^1$, corresponding to the boundary term along $y = 0$, turns out to be

$$\mathcal{B}^1 = \frac{1}{12h}\Big(\big\langle \hat{e}^{n+1}_{y_{-1}} - \hat{e}^{n+1}_{y_1}, \hat{e}^{n+1}_{y_1} \big\rangle_x + \frac{1}{2}\big\langle (\hat{e}^{n+1}_{y_{-2}} - \hat{e}^{n+1}_{y_2}) - 16(\hat{e}^{n+1}_{y_{-1}} - \hat{e}^{n+1}_{y_1}), \hat{e}^{n+1}_{y_0} \big\rangle_x \Big).$$

We focus on the estimate for $\mathcal{B}^1$, and the other three boundary terms $\mathcal{B}^2, \mathcal{B}^3, \mathcal{B}^4$ can be handled in a similar manner. Using the formula for $\hat{e}^{n+1}_{i,-1}$ and $\hat{e}^{n+1}_{i,-2}$ in (35), $\mathcal{B}^1$ can be simplified as

$$\begin{aligned} \mathcal{B}^1 &= -\frac{h^2}{36}\big\langle q^{n+1}_{y_0}, \hat{e}^{n+1}_{y_1} - 4\hat{e}^{n+1}_{y_0} \big\rangle_x \\ &\quad + \frac{1}{12h}\Big(\big\langle \xi^{n+1}_{y_0}, \hat{e}^{n+1}_{y_1} - 8\hat{e}^{n+1}_{y_0} \big\rangle_x + \frac{1}{2}\big\langle \zeta^{n+1}_{y_0}, \hat{e}^{n+1}_{y_0} \big\rangle_x \Big) \\ &\quad + \frac{h^4}{72}\big\langle p^{n+1}_{y_0}, \hat{e}^{n+1}_{y_0} - \hat{e}^{n+1}_{y_1} \big\rangle_x + \frac{h^4}{288}\big\langle r^{n+1}_{y_0}, \hat{e}^{n+1}_{y_0} - \hat{e}^{n+1}_{y_1} \big\rangle_x \\ &=: I_1 + I_2 + I_3 + I_4. \end{aligned} \tag{39}$$

The first term I_1 can be controlled by using the form of $q^{n+1}_{i,0}$ in (36):

$$\begin{aligned} &-\frac{h^2}{36}\big\langle q^{n+1}_{y_0}, \hat{e}^{n+1}_{y_1} \big\rangle_x \\ &= -\frac{h^2}{36}\big\langle (\partial_y b_1)_{y_0}(4\tilde{D}_x e^n_{y_1} - 2\tilde{D}_x e^n_{y_2} - 2\tilde{D}_x e^{n-1}_{y_1} + \tilde{D}_x e^{n-1}_{y_2}), \hat{e}^{n+1}_{y_1} \big\rangle_x \\ &\quad - \frac{h^2}{36}\big\langle (b_2)_{y_0}(4D_y^2 e^n_{y_1} - 2D_y^2 e^n_{y_2} - 2D_y^2 e^{n-1}_{y_1} + D_y^2 e^{n-1}_{y_2}), \hat{e}^{n+1}_{y_1} \big\rangle_x \end{aligned}$$

$$
\begin{aligned}
&-\frac{h^2}{36}\left\langle (\partial_y b_0)_{y_0}(2e^n_{y_0}-e^{n-1}_{y_0}), \hat{e}^{n+1}_{y_1}\right\rangle_x \\
&=:\ I_{1,1}+I_{1,2}+I_{1,3}.
\end{aligned}
$$

For $n \geq 5$, using (35) on the boundary segments $x = 0, 1$, the term $I_{1,1}$ can be bounded by

$$
\begin{aligned}
I_{1,1} &\leq h^4 \sum_{k=0}^{1}(|\tilde{D}_x \hat{e}^{n-k}_{0,1}|^2 + |\tilde{D}_x \hat{e}^{n-k}_{0,2}|^2 + |\tilde{D}_x \hat{e}^{n-k}_{N,1}|^2 + |\tilde{D}_x \hat{e}^{n-k}_{N,2}|^2) \\
&\quad + C_5\|\hat{e}^{n+1}\|_2^2 + C_5 h^2 \sum_{k=0}^{1}\|D_x e^{n-k}\|_2^2 + C_5 h^8 \\
&\leq C_6\|\hat{e}^{n+1}\|_2^2 + C_6 h^2 \sum_{k=0}^{1}\|D_x e^{n-k}\|_2^2 + C_6 h^6 \sum_{k=1}^{3}\|e^{n-k}\|_2^2 \\
&\quad + C_6 h^6 \sum_{k=1}^{3}\|D_y e^{n-k}\|_2^2 + C_6 h^6 \sum_{k=1}^{3}\|D_x^2 e^{n-k}\|_{2,n}^2 + C_6 h^8 \\
&\leq C_7 \sum_{k=-1}^{3}\|e^{n-k}\|_2^2 + C_7 h^2 \sum_{k=0}^{3}\|\nabla_h e^{n-k}\|_2^2 + C_7 h^6 \sum_{k=1}^{3}\|D_x^2\, e^{n-k}\|_{2,n}^2 + C_7 h^8,
\end{aligned}
\tag{40}
$$

in which the Schauder estimate (34) and the fact that $h \leq 1$ have been used. For $n = 3, 4$, the estimate (40) (with some constant C_7) could be similarly derived. The other two terms $I_{1,2}$ and $I_{1,3}$ can be handled by Cauchy's inequality:

$$
I_{1,2}+I_{1,3} \leq C_8 \sum_{k=-1}^{1}\|e^{n-k}\|_2^2 + \frac{h^2}{2304}\sum_{k=0}^{1}\|D_y^2 e^{n-k}\|_{2,n}^2 + C_8 h^8.
$$

A similar result is available for $\frac{h^2}{36}\left\langle q^{n+1}_{y_0}, 4\hat{e}^{n+1}_{y_0}\right\rangle_x$. Then we arrive at

$$
\begin{aligned}
I_1 &\leq C_9 \sum_{k=-1}^{3}\|e^{n-k}\|_2^2 + C_9 h^2 \sum_{k=0}^{3}\|\nabla_h e^{n-k}\|_2^2 + \frac{h^2}{1152}\sum_{k=0}^{1}\|D_y^2\, e^{n-k}\|_{2,n}^2 \\
&\quad + C_9 h^6 \sum_{k=1}^{3}\|D_x^2\, e^{n-k}\|_{2,n}^2 + C_9 h^8.
\end{aligned}
\tag{41}
$$

The term I_2 can be bounded with the help of Cauchy's inequality, as well as the estimate (36), giving

$$
I_2 \leq C_{10}\|\hat{e}^{n+1}\|_2^2 + C_{10}h^9 \leq C_{11}\|e^{n+1}\|_2^2 + C_{11}h^8. \tag{42}
$$

It remains to estimate I_3 and I_4. It is observed that, the detailed estimates for $\hat{e}^{n+1}_{i,-1}$, $\hat{e}^{n+1}_{i,-2}$ in (35), in which the $O(h^5)$ coefficients of $\hat{e}^{n+1}_{i,-1}$, $\hat{e}^{n+1}_{i,-2}$ have the ratio 1 : 14, enables a rewritten form of the term $I_3 + I_4$ as $\frac{h^4}{72}\left\langle p^{n+1}_{y_0}, \hat{e}^{n+1}_{y_0} - \hat{e}^{n+1}_{y_1}\right\rangle_x + \frac{h^4}{288}\left\langle r^{n+1}_{y_0}, \hat{e}^{n+1}_{y_0} - e^{n+1}_{y_1}\right\rangle_x$. This fact turns out to be crucial in the error analysis. An application of Cauchy's inequality implies that

$$
\begin{aligned}
I_3 + I_4 &= \frac{h^4}{72}\left\langle p^{n+1}_{y_0}, \hat{e}^{n+1}_{y_0} - \hat{e}^{n+1}_{y_1}\right\rangle_x + \frac{h^4}{288}\left\langle r^{n+1}_{y_0}, \hat{e}^{n+1}_{y_0} - \hat{e}^{n+1}_{y_1}\right\rangle_x \\
&\leq \frac{h}{97}\left\langle D_y^+\hat{e}^{n+1}_{y_0}, D_y^+\hat{e}^{n+1}_{y_0}\right\rangle_x + C_{12}h^{10}\sum_{i=0}^{N}(p^{n+1}_{i,0})^2 + C_{12}h^{10}\sum_{i=0}^{N}(r^{n+1}_{i,0})^2 \\
&\leq \frac{1}{97}\|D_y \hat{e}^{n+1}\|_2^2 + C_{13}h^9 \leq \frac{1}{96}\|D_y e^{n+1}\|_2^2 + C_{14}h^8.
\end{aligned}
\tag{43}
$$

A combination of (39) and (41)–(43) leads to

$$
\begin{aligned}
\mathcal{B}^1 &\leq C_{15}\sum_{k=-1}^{3}\|e^{n-k}\|_2^2 + \frac{1}{96}\|D_y e^{n+1}\|_2^2 + C_{15}h^2\sum_{k=0}^{3}\|\nabla_h e^{n-k}\|_2^2 \\
&\quad + \frac{h^2}{1152}\sum_{k=0}^{1}\|D_y^2\, e^{n-k}\|_{2,n}^2 + C_{15}h^6\sum_{k=1}^{3}\|D_x^2\, e^{n-k}\|_{2,n}^2 + C_{15}h^8.
\end{aligned}
$$

The other three boundary terms can be similarly treated, and we get

$$
\begin{aligned}
\mathcal{B} &\leq C_{16}\sum_{k=-1}^{3}\|e^{n-k}\|_2^2 + \frac{1}{48}\|\nabla_h e^{n+1}\|_2^2 + \frac{h^2}{576}\sum_{k=0}^{1}(\|D_x^2 e^{n-k}\|_{2,n}^2 + \|D_y^2 e^{n-k}\|_{2,n}^2) \\
&\quad + C_{16}h^2\sum_{k=0}^{3}\|\nabla_h e^{n-k}\|_2^2 + C_{16}h^6\sum_{k=1}^{3}(\|D_x^2\, e^{n-k}\|_{2,n}^2 + \|D_y^2\, e^{n-k}\|_{2,n}^2) \\
&\quad + C_{16}h^8.
\end{aligned}
\tag{44}
$$

A substitution of (44) into (38) gives

$$\begin{aligned}
&-\langle\big(\Delta_h-\frac{h^2}{12}(D_x^4+D_y^4)\big)\hat{e}^{n+1},\hat{e}^{n+1}\rangle\\
&\geq \frac{46}{48}\|\nabla_h e^{n+1}\|_2^2+\frac{47h^2}{576}(\|D_x^2\,e^{n+1}\|_{2,n}^2+\|D_y^2\,e^{n+1}\|_{2,n}^2)-C_{17}h^8\\
&\quad-\frac{h^2}{576}\sum_{k=0}^{1}(\|D_x^2\,e^{n-k}\|_{2,n}^2+\|D_y^2\,e^{n-k}\|_{2,n}^2)-C_{17}\sum_{k=-1}^{3}\|e^{n-k}\|_2^2\\
&\quad-C_{17}h^2\sum_{k=0}^{3}\|\nabla_h e^{n-k}\|_2^2-C_{17}h^6\sum_{k=1}^{3}(\|D_x^2\,e^{n-k}\|_{2,n}^2+\|D_y^2\,e^{n-k}\|_{2,n}^2).
\end{aligned}\tag{45}$$

To obtain (37), we make the following observation:

$$\begin{aligned}
&-\langle\big(\Delta_h-\frac{h^2}{12}(D_x^4+D_y^4)\big)\hat{e}^{n+1},\hat{e}^{n+1}\rangle\\
&=-\langle\big(\Delta_h-\frac{h^2}{12}(D_x^4+D_y^4)\big)e^{n+1},e^{n+1}\rangle\\
&\quad-h^4\langle\big(\Delta_h-\frac{h^2}{12}(D_x^4+D_y^4)\big)\hat{e}^{n+1},\hat{U}^{n+1}\rangle\\
&\quad-h^4\langle\big(\Delta_h-\frac{h^2}{12}(D_x^4+D_y^4)\big)\hat{U}^{n+1},e^{n+1}\rangle.
\end{aligned}\tag{46}$$

Regarding the second term on the right-hand side of (46), an application of the summation-by-parts formula, combined with (34), yields

$$\begin{aligned}
&-h^4\langle\big(\Delta_h-\frac{h^2}{12}(D_x^4+D_y^4)\big)\hat{e}^{n+1},\hat{U}^{n+1}\rangle\\
&\leq\frac{1}{48}\|\nabla_h e^{n+1}\|_2^2+\frac{h^2}{576}(\|D_x^2\,e^{n+1}\|_{2,n}^2+\|D_y^2\,e^{n+1}\|_{2,n}^2)+\mathcal{C}+C_{18}h^8.
\end{aligned}$$

Again, the boundary term is given by $\mathcal{C}=\mathcal{C}^1+\mathcal{C}^2+\mathcal{C}^3+\mathcal{C}^4$, and $\mathcal{C}^1$ (corresponding to the one along $y=0$) reads

$$\begin{aligned}
\mathcal{C}^1=&-\frac{1}{12h}\Big(\big\langle\hat{e}_{y_{-1}}^{n+1}-\hat{e}_{y_1}^{n+1},h^4\hat{U}_{y_1}^{n+1}\big\rangle_x\\
&+\frac{1}{2}\big\langle(\hat{e}_{y_{-2}}^{n+1}-\hat{e}_{y_2}^{n+1})-16(\hat{e}_{y_{-1}}^{n+1}-\hat{e}_{y_1}^{n+1}),h^4\hat{U}_{y_0}^{n+1}\big\rangle_x\Big).
\end{aligned}$$

For $n\geq 5$, the following bound is available, based on (35) and (36):

$$\mathcal{C}^1\leq C_{19}h^3\sum_{k=0}^{3}\Big(\|\nabla_h e^{n-k}\|_2^2+\|e^{n-k}\|_2^2+\|D_x^2\,e^{n-k}\|_{2,n}^2+\|D_y^2\,e^{n-k}\|_{2,n}^2\Big)+C_{19}h^8.$$

For $n=3,4$, the estimate with some alternate constant C_{19} can be derived in a similar manner. Moreover, the other three boundary terms, namely $\mathcal{C}^2$, $\mathcal{C}^3$, $\mathcal{C}^4$, can be similarly derived, and we arrive at

$$\begin{aligned}
&-h^4\langle(\Delta_h-\frac{h^2}{12}(D_x^4+D_y^4))\hat{e}^{n+1},\hat{U}^{n+1}\rangle\\
&\leq\frac{1}{48}\|\nabla_h e^{n+1}\|_2^2+\frac{h^2}{576}(\|D_x^2\,e^{n+1}\|_{2,n}^2+\|D_y^2\,e^{n+1}\|_{2,n}^2)+C_{20}h^8\\
&\quad+C_{20}h^3\sum_{k=0}^{3}\Big(\|\nabla_h e^{n-k}\|_2^2+\|e^{n-k}\|_2^2+\|D_x^2\,e^{n-k}\|_{2,n}^2+\|D_y^2\,e^{n-k}\|_{2,n}^2\Big).
\end{aligned}\tag{47}$$

Regarding the last term on the right-hand side of (46), we see that

$$-h^4\langle\big(\Delta_h-\frac{h^2}{12}(D_x^4+D_y^4)\big)\hat{U}^{n+1},e^{n+1}\rangle\leq C_{21}\|e^{n+1}\|_2^2+C_{21}h^8.\tag{48}$$

Finally, a combination of (45)–(48) gives (37), which completes the proof. □

Proposition 2. *The following inequality is valid for $n\geq 3$ and $m=1,3$:*

$$\begin{aligned}
&|\langle\big(\Delta_h-\frac{h^2}{12}(D_x^4+D_y^4)\big)e^{n-m},e^{n+1}\rangle|\\
&\leq\frac{25}{48}\|\nabla_h e^{n+1}\|_2^2+\frac{27}{48}\|\nabla_h e^{n-m}\|_2^2+\frac{25h^2}{576}(\|D_x^2\,e^{n+1}\|_{2,n}^2+\|D_y^2\,e^{n+1}\|_{2,n}^2)\\
&\quad+\frac{26h^2}{576}(\|D_x^2\,e^{n-m}\|_{2,n}^2+\|D_y^2\,e^{n-m}\|_{2,n}^2)+C_{29}\|e^{n+1}\|_2^2+C_{29}h^8\\
&\quad+\frac{h^2}{576}\sum_{k=m+1}^{m+2}(\|D_x^2e^{n-k}\|_{2,n}^2+\|D_y^2e^{n-k}\|_{2,n}^2)+C_{29}\sum_{k=m+1}^{m+4}\|e^{n-k}\|_2^2
\end{aligned}$$

$$+ C_{29}h^2 \sum_{k=m+1}^{m+4} \|\nabla_h e^{n-k}\|_2^2 + C_{29}h^3 \sum_{k=m+1}^{m+4} (\|D_x^2 e^{n-k}\|_{2,n}^2 + \|D_y^2 e^{n-k}\|_{2,n}^2). \tag{49}$$

The estimate for the convection terms in (18) is stated in the following proposition.

Proposition 3. *The following inequality is valid for $n \geq 3$:*

$$\begin{aligned}
&\left\langle \frac{23}{6}\boldsymbol{b}\cdot\nabla_{h,(4)}e^n - \frac{8}{3}\boldsymbol{b}\cdot\nabla_{h,(4)}e^{n-1} + \frac{5}{6}\boldsymbol{b}\cdot\nabla_{h,(4)}e^{n-2}, e^{n+1}\right\rangle \\
&\leq \frac{1}{48}\sum_{k=0}^{2}\|\nabla_h e^{n-k}\|_2^2 + C_{31}\|e^{n+1}\|_2^2 + C_{31}h^8 \\
&\quad + C_{31}h^4\sum_{k=1}^{4}(\|e^{n-k}\|_2^2 + \|\nabla_h e^{n-k}\|_2^2 + \|D_x^2 e^{n-k}\|_{2,n}^2 + \|D_y^2 e^{n-k}\|_{2,n}^2).
\end{aligned} \tag{50}$$

Proof. We focus on the term $\langle \boldsymbol{b}\cdot\nabla_{h,(4)}e^n, e^{n+1}\rangle$, and the rest two terms could be similarly treated. An application of the summation-by-parts formula indicates that

$$\begin{aligned}
&\langle b_1\tilde{D}_x(1-\frac{h^2}{6}D_x^2)e^n, e^{n+1}\rangle + \langle b_2\tilde{D}_y(1-\frac{h^2}{6}D_y^2)e^n, e^{n+1}\rangle \\
&= \frac{4h}{3}\sum_{i=1}^{N-1}\langle (b_1)_{x_i}\tilde{D}_x e^n_{x_i}, e^{n+1}_{x_i}\rangle_y - \frac{h}{6}\sum_{i=2}^{N-1}\langle (b_1)_{x_i}\tilde{D}_x e^n_{x_{i-1}}, e^{n+1}_{x_i}\rangle_y \\
&\quad - \frac{h}{6}\sum_{i=1}^{N-2}\langle (b_1)_{x_i}\tilde{D}_x e^n_{x_{i+1}}, e^{n+1}_{x_i}\rangle_y + \frac{4h}{3}\sum_{j=1}^{N-1}\langle (b_2)_{y_j}\tilde{D}_y e^n_{y_j}, e^{n+1}_{y_j}\rangle_x \\
&\quad - \frac{h}{6}\sum_{i=2}^{N-1}\langle (b_2)_{y_j}\tilde{D}_y e^n_{y_{j-1}}, e^{n+1}_{y_j}\rangle_x - \frac{h}{6}\sum_{i=1}^{N-2}\langle (b_2)_{y_j}\tilde{D}_y e^n_{y_{j+1}}, e^{n+1}_{y_j}\rangle_x + \mathcal{A} \\
&\leq \frac{6}{23}\cdot\frac{1}{48}\|\nabla_h e^n\|_2^2 + C_{23}\|e^{n+1}\|_2^2 + \mathcal{A}.
\end{aligned}$$

The boundary term $\mathcal{A}$ can be decomposed as $\mathcal{A} = \mathcal{A}^1 + \mathcal{A}^2 + \mathcal{A}^3 + \mathcal{A}^4$, in which $\mathcal{A}^1$ (corresponding to the one along $y = 0$) is given by

$$\begin{aligned}
\mathcal{A}^1 &= \frac{2}{3}\langle (b_2)_{y_0}(e^n_{y_1} - e^n_{y_{-1}}), e^{n+1}_{y_0}\rangle_x - \frac{1}{6}\langle (b_2)_{y_1}(e^n_{y_1} - e^n_{y_{-1}}), e^{n+1}_{y_1}\rangle_x \\
&\quad - \frac{1}{12}\langle (b_2)_{y_0}(e^n_{y_2} - e^n_{y_{-2}}), e^{n+1}_{y_0}\rangle_x.
\end{aligned} \tag{51}$$

For $n \geq 4$, an insertion of (31) into (30), combined with a subtraction from (11), results in

$$\begin{aligned}
e^n_{i,-1} - e^n_{i,1} &= \frac{h^3}{3}q^n_{i,0} + \phi^n_{i,0}, \quad \text{with } |\phi^n_{i,0}| \leq Ch^5\|U\|_{W^{3,\infty}(0,T;C^{7,\alpha})}, \\
e^n_{i,-2} - e^n_{i,2} &= \frac{8h^3}{3}q^n_{i,0} + \psi^n_{i,0}, \quad \text{with } |\psi^n_{i,0}| \leq Ch^5\|U\|_{W^{3,\infty}(0,T;C^{7,\alpha})}.
\end{aligned} \tag{52}$$

Additionally, a combination of (52) and the a-priori estimate (17) yields

$$|\tilde{D}_y e^n_{i,0}| \leq h, \quad \text{for } h < C_\star \text{ (independent of } \Delta t \text{ and } h). \tag{53}$$

Meanwhile, both (52) and (53) can be extended to the other three boundary segments.

The first term of $\mathcal{A}^1$ could be bounded with the help of (52):

$$\langle (b_2)_{y_0}(e^n_{y_1} - e^n_{y_{-1}}), e^{n+1}_{y_0}\rangle_x \leq \frac{h^3}{3}\langle (b_2)_{y_0}q^{n+1}_{y_0}, e^{n+1}_{y_0}\rangle_x + C_{24}\|e^{n+1}\|_2^2 + C_{24}h^8, \tag{54}$$

with an obvious fact $h \leq 1$. Subsequently, we see that

$$\begin{aligned}
&\frac{h^3}{3}\langle (b_2)_{y_0}q^n_{y_0}, e^{n+1}_{y_0}\rangle_x \\
&= \frac{h^3}{3}\langle (b_2)_{y_0}(\partial_y b_1)_{y_0}(4\tilde{D}_x e^{n-1}_{y_1} - 2\tilde{D}_x e^{n-1}_{y_1} - 2\tilde{D}_x e^{n-2}_{y_2} + \tilde{D}_x e^{n-2}_{y_1}), e^{n+1}_{y_0}\rangle_x \\
&\quad + \frac{h^3}{3}\langle (b_2)_{y_0}(b_2)_{y_0}(4D_y^2 e^{n-1}_{y_1} - 2D_y^2 e^{n-1}_{y_2} - 2D_y^2 e^{n-2}_{y_1} + D_y^2 e^{n-2}_{y_2}), e^{n+1}_{y_0}\rangle_x \\
&\quad + \frac{h^3}{3}\langle (b_2)_{y_0}(\partial_y b_0)_{y_0}(2e^{n-1}_{y_0} - e^{n-2}_{y_0}), e^{n+1}_{y_0}\rangle_x =: \Phi_1 + \Phi_2 + \Phi_3.
\end{aligned} \tag{55}$$

Using (52) on the boundary segments $x = 0, 1$, we have

$$\Phi_1 \leq \frac{h^4}{6}(b_2)_{0,0}(\partial_y b_1)_{0,0}(4\tilde{D}_x e^{n-1}_{0,1} - 2\tilde{D}_x e^{n-1}_{0,2} - 2\tilde{D}_x e^{n-2}_{0,1} + \tilde{D}_x e^{n-2}_{0,2})e^{n+1}_{0,0}$$

$$
\begin{aligned}
&+\frac{h^4}{6}(b_2)_{N,0}(\partial_y b_1)_{N,0}(4\tilde{D}_x e^{n-1}_{N,1}-2\tilde{D}_x e^{n-1}_{N,2}-2\tilde{D}_x e^{n-2}_{N,1}+\tilde{D}_x e^{n-2}_{N,2})e^{n+1}_{N,0}\\
&+C_{25}\|e^{n+1}\|_2^2+C_{25}h^4\|D_x e^{n-1}\|_2^2+C_{25}h^4\|D_x e^{n-2}\|_2^2\\
\le{}& C_{26}\|e^{n+1}\|_2^2+C_{26}h^4\|D_x e^{n-1}\|_2^2+C_{26}h^4\|D_x e^{n-2}\|_2^2+C_{26}h^8,
\end{aligned}
\tag{56}
$$

in which the estimate (53) on the boundary segments $x = 0, 1$ has been used. The terms Φ_2, Φ_3 can be directly controlled by Cauchy's inequality, giving

$$
\Phi_2 \le C_{27}\|e^{n+1}\|_2^2+C_{27}h^4\|D_y^2 e^{n-1}\|_{2,n}^2+C_{27}h^4\|D_y^2 e^{n-2}\|_{2,n}^2, \tag{57}
$$

$$
\Phi_3 \le C_{27}\|e^{n+1}\|_2^2+C_{27}h^4\|e^{n-1}\|_2^2+C_{27}h^4\|e^{n-2}\|_2^2. \tag{58}
$$

A combination of (54)–(58) implies that there exists a constant C_{28} such that

$$
\begin{aligned}
&\frac{2}{3}\langle (b_2)_{y_0}(e^n_{y_1}-e^n_{y_{-1}}), e^{n+1}_{y_0}\rangle_x\\
&\le C_{28}h^4\sum_{k=1}^{2}(\|e^{n-k}\|_2^2+\|D_x e^{n-k}\|_2^2+\|D_y^2 e^{n-k}\|_{2,n}^2)\\
&\quad + C_{28}\|e^{n+1}\|_2^2+C_{28}h^8.
\end{aligned}
\tag{59}
$$

For $n = 3$, this inequality (with some constant C_{28}) could be similarly derived.

The estimates of the other two terms in (51) can be derived in the same fashion, giving

$$
\mathcal{A}^1 \le C_{29}\Big(\|e^{n+1}\|_2^2+h^8+h^4\sum_{k=1}^{2}(\|e^{n-k}\|_2^2+\|D_x e^{n-k}\|_2^2+\|D_y^2 e^{n-k}\|_{2,n}^2)\Big).
$$

The other three boundary terms can be similarly treated, and we get

$$
\begin{aligned}
&\langle b_1\tilde{D}_x(1-\frac{h^2}{6}D_x^2)e^n, e^{n+1}\rangle+\langle b_2\tilde{D}_y(1-\frac{h^2}{6}D_y^2)e^n, e^{n+1}\rangle\\
&\le \frac{6}{23}\cdot\frac{1}{48}\|\nabla_h e^n\|_2^2+C_{30}\|e^{n+1}\|_2^2+C_{30}h^8\\
&\quad + C_{30}h^4\sum_{k=1}^{2}(\|e^{n-k}\|_2^2+\|\nabla_h e^{n-k}\|_2^2+\|D_x^2 e^{n-k}\|_{2,n}^2+\|D_y^2 e^{n-k}\|_{2,n}^2).
\end{aligned}
$$

The proof is completed. □

Finally, a substitution of (19)–(21), (24)–(26), (37), (49) and (50) into (18) results in

$$
\begin{aligned}
&\|e^{n+1}\|_2^2-\|e^n\|_2^2\\
&\quad+\Delta t\big(\frac{35}{48}\|\nabla_h e^{n+1}\|_2^2-\frac{1}{48}\|\nabla_h e^{n}\|_2^2-\frac{47}{96}\|\nabla_h e^{n-1}\|_2^2-\frac{1}{48}\|\nabla_h e^{n-2}\|_2^2-\frac{3}{32}\|\nabla_h e^{n-3}\|_2^2\big)\\
&\quad+\Delta t\frac{109h^2}{1728}(\|D_x^2 e^{n+1}\|_{2,n}^2+\|D_y^2 e^{n+1}\|_{2,n}^2)-\Delta t\frac{65h^2}{1728}(\|D_x^2 e^{n-1}\|_{2,n}^2+\|D_y^2 e^{n-1}\|_{2,n}^2)\\
&\quad-\Delta t\frac{13h^2}{1728}(\|D_x^2 e^{n-3}\|_{2,n}^2+\|D_y^2 e^{n-3}\|_{2,n}^2)-\Delta t\frac{h^2}{576}\sum_{k=0}^{5}(\|D_x^2 e^{n-k}\|_{2,n}^2+\|D_y^2 e^{n-k}\|_{2,n}^2)\\
&\le C_{32}\Delta t h^2\sum_{k=0}^{7}\|\nabla_h e^{n-k}\|_2^2+C_{32}\Delta t h^3\sum_{k=0}^{7}(\|D_x^2 e^{n-k}\|_{2,n}^2+\|D_y^2 e^{n-k}\|_{2,n}^2)\\
&\quad+C_{32}\Delta t\sum_{k=-1}^{7}\|e^{n-k}\|_2^2+C_{32}\Delta t\sum_{k=1}^{3}\sum_{r=0}^{2}\|e^{m_{n-r}-k}\|_2^2+\Delta t\|\tau^{n+1}\|_2^2+C_{32}\Delta t h^8.
\end{aligned}
\tag{60}
$$

For any $0 < k_* < k^* \le N_t$ such that $\theta(t_{k^*})-\theta(t_{k_*}) \le 3\Delta t$, one has $\theta'(\rho)(k^*-k_*)\Delta t \le 3\Delta t$ where $\rho \in [k_*\Delta t, k^*\Delta t]$, which implies that $k^*-k_* \le \frac{3}{\min\theta'}$. Therefore, we get

$$
\sum_{k=1}^{3}\sum_{r=0}^{2}\|e^{m_{n-r}-k}\|_2^2 \le \frac{27}{\min\theta'}\sum_{k=0}^{n}\|e^k\|_2^2. \tag{61}
$$

Consequently, choosing $h \le \min\{(96C_{32})^{-\frac{1}{2}}, 5\cdot(6912C_{32})^{-1}\}$, summing up (60) in time, using (61), (A.10), and the fact that $\frac{35}{48}-\frac{1}{48}-\frac{47}{96}-\frac{1}{48}-\frac{3}{32}-\frac{8}{96}=\frac{1}{48}>0$, $\frac{109}{1728}-\frac{65}{1728}-\frac{13}{1728}-\frac{6}{576}-\frac{8\cdot5}{6912}=\frac{1}{12\cdot48}>0$, we see that an application of discrete Gronwall inequality gives the desired error estimate:

$$
\|e^{n+1}\|_2^2+\frac{\Delta t}{48}\sum_{k=4}^{n+1}\big(\|\nabla_h e^k\|_2^2+\frac{h^2}{12}(\|D_x^2 e^k\|_{2,n}^2+\|D_y^2 e^k\|_{2,n}^2)\big) \le C_{33}(\Delta t^3+h^4)^2. \tag{62}
$$

2.2.4. Recovery of the prior ℓ^∞ bound (17)

Finally, an application of the inverse inequality to the ℓ^2 error estimate (62) yields

$$\|e^{n+1}\|_\infty \le 2h^{-1}\|e^{n+1}\|_2 \le 2C_{33}^{\frac{1}{2}} h^{-1}(\Delta t^3 + h^4) \le 2C_{33}^{\frac{1}{2}}(\tilde{C}^3 h^2 + h^3),$$

in which we have used the linear refinement requirement $\Delta t \le \tilde{C}h$ in the derivation. Setting $h \le \min\{1, (2C_{33}^{\frac{1}{2}}(\tilde{C}^3+1))^{-2}\}$, we see that the prior ℓ^∞ bound of $\|e^{n+1}\|_\infty \le h^{\frac{3}{2}}$ is recovered.

Remark 1. For the Dirichlet boundary condition case, one would need a different ghost-point construction and a separate boundary truncation error analysis from the Neumann case studied in this paper; hence the arguments developed here cannot be directly adapted. Similarly, a symmetric extrapolation for the ghost point can be used so that the resulting scheme can still be solved efficiently by the FFT-based method. We expect the theoretical convergence rate to be $O(\Delta t^3 + h^{3.5})$ based on the analysis in [26], while the full accuracy of $O(\Delta t^3 + h^4)$ is anticipated in practical computations [27]. A complete and rigorous proof for the Dirichlet case would require a separate technical development and is therefore left to the interested reader.

3. The fourth-order multi-step scheme

It is observed that the Adams–Moulton formula applied to the diffusion term in the third-order multi-step scheme (6) is a stretched stencil, and that the diffusion coefficient at time step t_{n+1} dominates the sum of the remaining coefficients, which plays a key role for the stability and convergence analysis in Section 2. This property is a necessary condition for the numerical stability; see the related discussions in [32–34]. Directly applying the classical Adams–Moulton formula (cf. [36]) to the diffusion term and Adams–Bashforth formula to the convection term, linear reaction term and nonlinear function results in the following third- and fourth-order multi-step linearized schemes:

$$\begin{aligned}
\text{Third order:}\quad & \frac{u^{n+1}-u^n}{\Delta t} - \Delta_{h,(4)}\Big(\frac{5}{12}u^{n+1} + \frac{2}{3}u^n - \frac{1}{12}u^{n-1}\Big)\\
&= \frac{23}{12}\Big(f(\tilde{u}_\theta^n, u^n) - \boldsymbol{b}\cdot\nabla_{h,(4)}u^n - b_0u^n\Big)\\
&\quad - \frac{4}{3}\Big(f(\tilde{u}_\theta^{n-1}, u^{n-1}) - \boldsymbol{b}\cdot\nabla_{h,(4)}u^{n-1} - b_0u^{n-1}\Big)\\
&\quad + \frac{5}{12}\Big(f(\tilde{u}_\theta^{n-2}, u^{n-2}) - \boldsymbol{b}\cdot\nabla_{h,(4)}u^{n-2} - b_0u^{n-2}\Big), \qquad (63)\\
\text{Fourth order:}\quad & \frac{u^{n+1}-u^n}{\Delta t} - \Delta_{h,(4)}\Big(\frac{9}{24}u^{n+1} + \frac{19}{24}u^n - \frac{5}{24}u^{n-1} + \frac{1}{24}u^{n-2}\Big)\\
&= \frac{55}{24}\Big(f(\tilde{u}_\theta^n, u^n) - \boldsymbol{b}\cdot\nabla_{h,(4)}u^n - b_0u^n\Big)\\
&\quad - \frac{59}{24}\Big(f(\tilde{u}_\theta^{n-1}, u^{n-1}) - \boldsymbol{b}\cdot\nabla_{h,(4)}u^{n-1} - b_0u^{n-1}\Big)\\
&\quad + \frac{37}{24}\Big(f(\tilde{u}_\theta^{n-2}, u^{n-2}) - \boldsymbol{b}\cdot\nabla_{h,(4)}u^{n-2} - b_0u^{n-2}\Big)\\
&\quad - \frac{3}{8}\Big(f(\tilde{u}_\theta^{n-3}, u^{n-3}) - \boldsymbol{b}\cdot\nabla_{h,(4)}u^{n-3} - b_0u^{n-3}\Big), \qquad (64)
\end{aligned}$$

and the numerical results in Section 4.3 reveal that these schemes are unstable. Therefore, a stretched Adams–Moulton formula is also needed for the fourth-order multi-step linearized scheme, which is formulated as follows:

$$\begin{aligned}
&\frac{u^{n+1}-u^n}{\Delta t} - \Delta_{h,(4)}\Big(\frac{757}{1152}u^{n+1} + \frac{470}{1152}u^{n-1} - \frac{118}{1152}u^{n-5} + \frac{43}{1152}u^{n-7}\Big)\\
&= \frac{55}{24}\Big(f(\tilde{u}_\theta^n, u^n) - \boldsymbol{b}\cdot\nabla_{h,(4)}u^n - b_0u^n\Big)\\
&\quad - \frac{59}{24}\Big(f(\tilde{u}_\theta^{n-1}, u^{n-1}) - \boldsymbol{b}\cdot\nabla_{h,(4)}u^{n-1} - b_0u^{n-1}\Big)\\
&\quad + \frac{37}{24}\Big(f(\tilde{u}_\theta^{n-2}, u^{n-2}) - \boldsymbol{b}\cdot\nabla_{h,(4)}u^{n-2} - b_0u^{n-2}\Big)\\
&\quad - \frac{3}{8}\Big(f(\tilde{u}_\theta^{n-3}, u^{n-3}) - \boldsymbol{b}\cdot\nabla_{h,(4)}u^{n-3} - b_0u^{n-3}\Big),
\end{aligned} \qquad (65)$$

for $n \ge 7$, where $u^0 = U_0$. Here, $\tilde{u}_\theta^n := \sum_{i=1}^4 u^{m_n-i}\prod_{j\ne i}^{1\le j\le 4}\frac{\theta(t_n)-t_{m_n-j}}{t_{m_n-i}-t_{m_n-j}}$ is an explicit approximation to $U(\theta(t_n))$, where

$$m_n := \begin{cases} 4 & \text{if } 0 < \theta(t_n) \le 3\Delta t,\\ q & \text{if } (q-1)\Delta t < \theta(t_n) \le q\Delta t \text{ for some } q > 3.\end{cases}$$

The formula for the ghost points near the boundary $y = 0$ is given by (11). Moreover, the initial values of u^n for $n = 1, 2, \dots, 7$, must also be computed with temporal error of $O(\Delta t^4)$, and the predictor-corrector method could still be considered here.

For the fourth-order multi-step linearized scheme (65), the convergence estimate is stated below.

Table 1
ℓ^2 and ℓ^∞ errors norms of scheme (6) with $\Delta t = 10^{-3}$.

	$\theta(t)=0.8t$				$\theta(t)=\arctan t$			
h	$\|u^{N_t}-U_e^{N_t}\|_2$	Order	$\|u^{N_t}-U_e^{N_t}\|_\infty$	Order	$\|u^{N_t}-U_e^{N_t}\|_2$	Order	$\|u^{N_t}-U_e^{N_t}\|_\infty$	Order
2^{-4}	8.4533e-05	–	1.9905e-04	–	8.6015e-05	–	2.0089e-04	–
2^{-5}	5.6272e-06	3.9090	1.2657e-05	3.9752	5.7375e-06	3.9061	1.2790e-05	3.9734
2^{-6}	3.5963e-07	3.9678	7.9398e-07	3.9947	3.6697e-07	3.9667	8.0270e-07	3.9940
2^{-7}	2.4110e-08	3.8988	5.1364e-08	3.9503	2.4676e-08	3.8945	5.2013e-08	3.9479

Table 2
ℓ^2 and ℓ^∞ errors of scheme (6) with $h = 10^{-3}$.

	$\theta(t)=0.8t$				$\theta(t)=\arctan t$			
Δt	$\|u^{N_t}-U_e^{N_t}\|_2$	Order	$\|u^{N_t}-U_e^{N_t}\|_\infty$	Order	$\|u^{N_t}-U_e^{N_t}\|_2$	Order	$\|u^{N_t}-U_e^{N_t}\|_\infty$	Order
2^{-6}	6.3099e-06	–	7.9122e-06	–	6.6042e-06	–	8.1519e-06	–
2^{-7}	8.7047e-07	2.8578	1.0695e-06	2.8872	9.1695e-07	2.8485	1.1077e-06	2.8795
2^{-8}	1.1341e-07	2.9402	1.3822e-07	2.9518	1.1978e-07	2.9364	1.4355e-07	2.9479
2^{-9}	1.4740e-08	2.9437	1.7825e-08	2.9550	1.5591e-08	2.9416	1.8546e-08	2.9524

Theorem 2. *Assume that $f = f(v_1, v_2) \in C^4(\mathbb{R}^2)$ and $\theta \in C^4[0,T]$. Let $U \in W^{4,\infty}(0,T; C^{7,\alpha}(\overline{\Omega}))$ be the exact solution of the delay CDR equation (1)–(3), and u^n be the fully discrete numerical solution obtained by (65). As $\Delta t, h \to 0$ under a linear refinement requirement $\Delta t \le \tilde{C} h$, we obtain the following result: for $n = 1, 2, \ldots, N_t$,*

$$\|u^n - U^n\|_2 \le C(\Delta t^4 + h^4), \quad \text{with } C \text{ independent of } \Delta t \text{ and } h.$$

Proof. The procedure of the proof is identical to that of Theorem 1, with only minor differences arising from the specific coefficients in the Adams formulas. Since the diffusion coefficient at time level t_{n+1} in scheme (65) dominates the sum of the remaining diffusion coefficients, the coefficient of $\|\nabla e^{n+1}\|_2^2$ remains dominant over the sum of the coefficients of $\|\nabla e^{n-k}\|_2^2$. We omit the redundant derivation and leave the details to the interested reader. □

Remark 2. The time stencil in scheme (65) is essentially minimal for achieving fourth-order accuracy together with unconditional stability with respect to the diffusion term. Indeed, the stability proof relies on an Adams–Moulton representation

$$\frac{1}{\Delta t}\int_{t_n}^{t_{n+1}} \Delta U(t)\,dt = a_0 \Delta U(t_{n+1}) + \sum_{i=1}^{3} a_{j(i)} \Delta U(t_{n-j(i)}) + C\Delta t^4$$

with condition $a_0 > \sum_i |a_{j(i)}|$. Detailed calculations show that the shortest admissible choice is $j(1) = 1$, $j(2) = 5$, $j(3) = 7$.

4. The numerical results

In this section, some numerical examples are provided to demonstrate the robustness of the proposed schemes. The following two dimensional convection-diffusion-reaction equation is taken into consideration, with a vanishing delay term:

$$\partial_t U - \Delta U + \boldsymbol{b} \cdot \nabla U + b_0 U = f(U(\theta(t)), U(t)) + g, \quad (\boldsymbol{x}, t) \in (0,1)^2 \times [0,1]. \tag{66}$$

We take the nonlinear function $f(U(\theta(t)), U(t)) = U(\theta(t))U^2(t)$ and set $\boldsymbol{b} = (1,1)^T$, $b_0 = 1$. Two types of delay functions: the linear delay function $\theta(t) = 0.8t$ and the nonlinear delay function $\theta(t) = \arctan t$ are considered. The exact solution is chosen as $U_e = \cos(t\cos(\pi x)\cos(\pi y))$. The initial data is given by $U_e(\boldsymbol{x}, 0) = 1$, and the source term g is accordingly determined. The three-point Simpson's integration formula is used for g to minimize the numerical integration error over each time interval (t_n, t_{n+1}). Both the third- and fourth-order schemes can be efficiently solved via FFT.

4.1. Numerical test for the third-order scheme

To verify the spatial accuracy of the third-order scheme (6), the time step size Δt is needed to be sufficiently small to ensure the numerical error is dominated by the spatial error. In this test, we fix $\Delta t = 10^{-3}$. In Table 1, the spatial numerical errors of scheme (6) are presented. It is apparent that the convergence rate in both the ℓ^2 and ℓ^∞ norms are close to $O(h^4)$, whatever the delay function $\theta(t)$ is linear or nonlinear.

To verify the temporal accuracy, the spatial mesh size h has to be sufficiently small to ensure the spatial numerical error is negligible, and we fix $h = 10^{-3}$. In Table 2, the associated numerical errors are presented. It is obvious that the convergence rate in both the ℓ^2 and ℓ^∞ norms are close to $O(\Delta t^3)$, whatever the delay function $\theta(t)$ is linear or nonlinear.

Table 3
ℓ^2 and ℓ^∞ errors of scheme (65) with $\Delta t = h$.

		$\theta(t) = 0.8t$				$\theta(t) = \arctan t$			
Δt	h	$\|u^{N_t} - U_e^{N_t}\|_2$	Order	$\|u^{N_t} - U_e^{N_t}\|_\infty$	Order	$\|u^{N_t} - U_e^{N_t}\|_2$	Order	$\|u^{N_t} - U_e^{N_t}\|_\infty$	Order
2^{-4}	2^{-4}	6.6775e-05	–	1.7587e-04	–	6.3431e-05	–	1.7101e-04	–
2^{-5}	2^{-5}	5.1702e-06	3.6910	1.2255e-05	3.8430	4.9798e-06	3.6710	1.2040e-05	3.8282
2^{-6}	2^{-6}	3.5338e-07	3.8709	7.9579e-07	3.9449	3.5487e-07	3.8107	7.9900e-07	3.9134
2^{-7}	2^{-7}	2.2935e-08	3.9456	5.0526e-08	3.9773	2.3680e-08	3.9056	5.1466e-08	3.9565

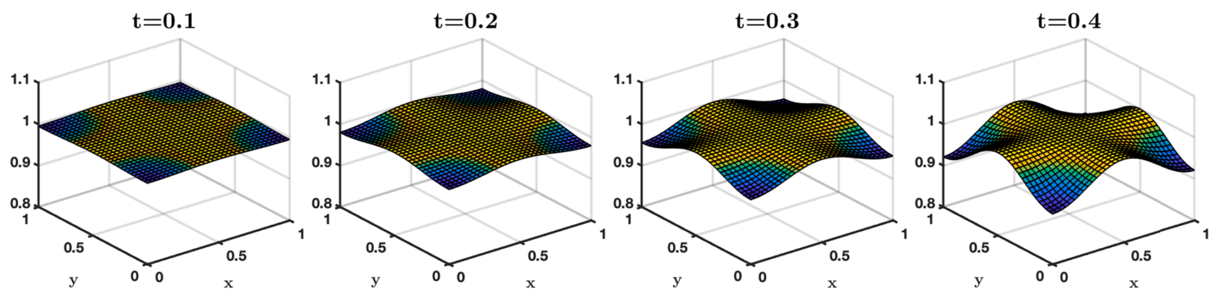

Fig. 1. The numerical solution of the third-order multi-step linearized scheme (6) with stretched Adams–Bashforth formula.

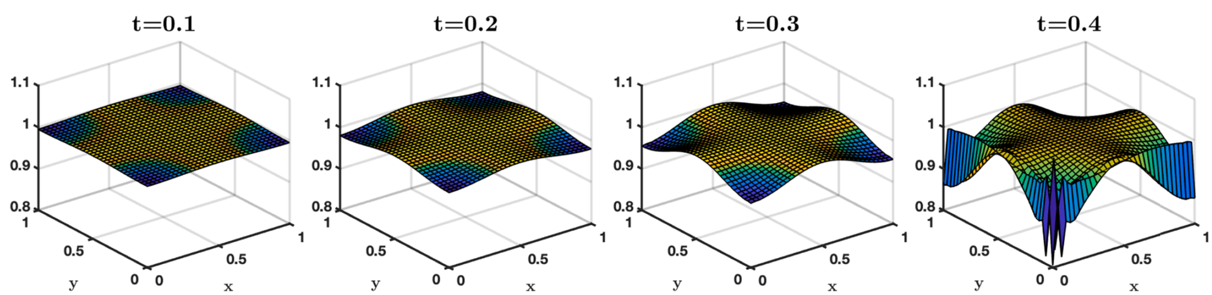

Fig. 2. The numerical solution of the third-order multi-step linearized scheme (63) with classical Adams–Bashforth formula.

4.2. Numerical test for the fourth-order scheme

To verify the numerical accuracy of the fourth-order scheme (65), the time step size is set as $\Delta t = h$ so that the fourth-order accuracy in both time and space can be confirmed. The numerical results are presented in Table 3, and the desired fourth-order convergence rate is clearly observed.

4.3. The instability of scheme (63) and (64)

It is observed that the diffusion coefficient at time step t_{n+1} in scheme (6) dominates the sum of the rest of diffusion coefficients, i.e., $\frac{2}{3} > |\frac{5}{12}| + |\frac{1}{12}|$. This fact has played a crucial role in our stability and convergence analysis. However, the scheme (63), obtained by applying the classical Adams–Moulton formula to the diffusion term, does not possess this property. For comparison, we present in Figs. 1 and 2 the numerical solutions of (66) obtained with the two schemes. The computation is performed with $h = 1/2^5$, $\Delta t = 0.01$, and the nonlinear delay is taken as $\theta(t) = \arctan t$. The exact solution is displayed in Fig. 5. The instability of the scheme (63) is easily observed. The numerical solutions obtained using schemes (65) and (64) are shown in Figs. 3 and 4, respectively. Instability is also observed in the scheme (64).

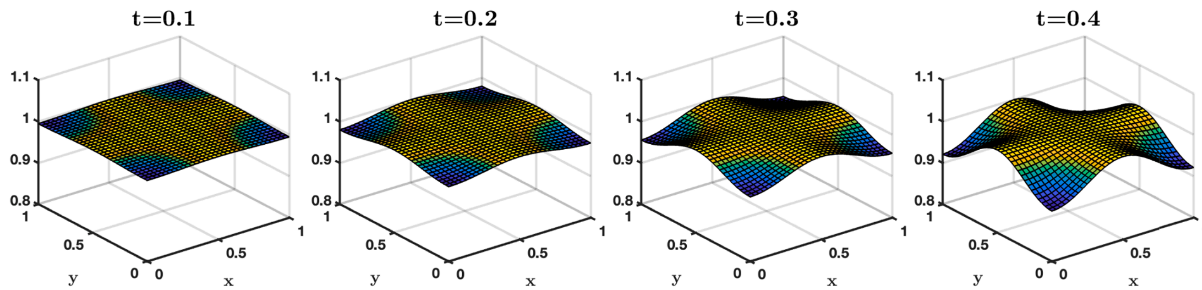

Fig. 3. The numerical solution of the fourth-order multi-step linearized scheme (65) with stretched Adams–Bashforth formula.

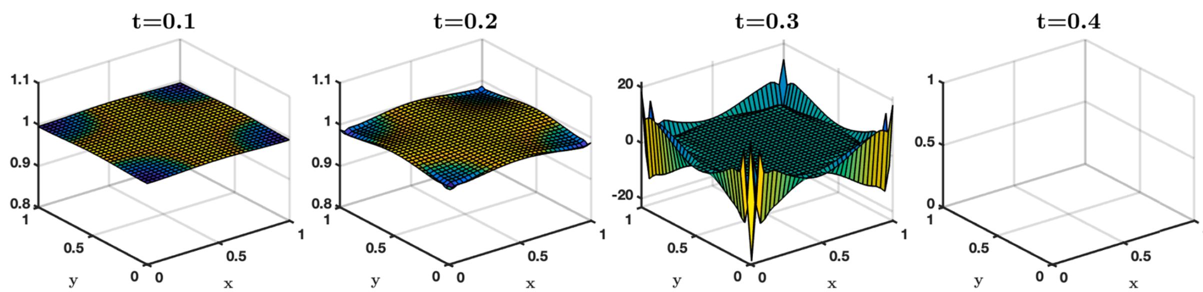

Fig. 4. The numerical solution of the fourth-order multi-step linearized scheme (64) with classical Adams–Bashforth formula. The numerical solution blows up at $t = 0.4$.

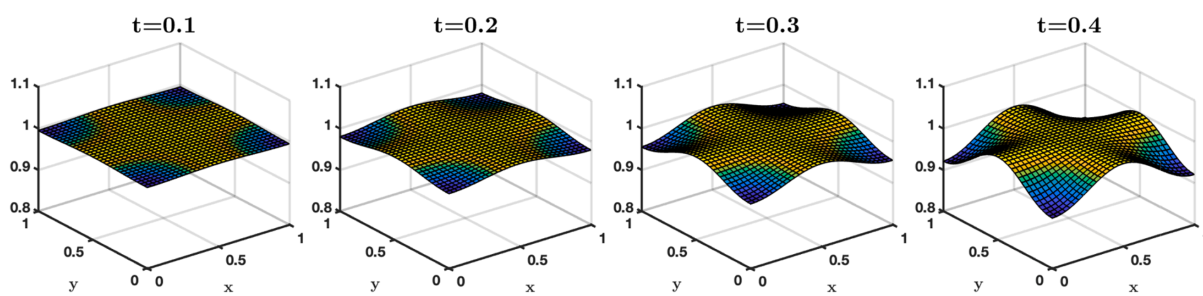

Fig. 5. The exact solution $U_e = \cos(t\cos(\pi x)\cos(\pi y))$.

5. Colclusion

In this paper, two multi-step, linearized numerical schemes, by virtue of a combination of the Adams–Bashforth extrapolation and the stretched Adams–Moulton interpolation in the temporal discretization, are proposed to solve the CDR equation with vanishing delay. The fourth-order long-stencil finite difference formula is used for the spatial discretization, and the boundary extrapolation is implemented by making use of Taylor expansions and information from the delay CDR equation. A detailed convergence analysis and error estimate is provided for the proposed numerical scheme. Via a careful construction of an approximated solution, we obtain the full order accuracy estimate in the ℓ^2 norm. The numerical experiments have also verified the theoretical analysis. Additionally, a potential future direction is to investigate the preservation of physical structures, such as the discrete maximum principle, and to explore superconvergence properties [37,38].

Data availability

No data was used for the research described in the article.

Declaration of competing interest

The authors declare that they have no known competing financial interests or personal relationships that could have appeared to influence the work reported in this paper.

Acknowledgement

This work is supported in part by NSFC 12371385 (Q. Huang) and NSF DMS-2012269, DMS-2309548 (C. Wang).

Appendix A. Estimates of the starting approximations

We first analyze the error $e^1_{[1]} := U^1 - u^1_{[1]}$ caused by the predictor. A careful consistency analysis implies that

$$\frac{U^1 - U^0}{\Delta t} - \Delta_{h,(4)} U^1 = f(U^0, U^0) - \boldsymbol{b} \cdot \nabla_{h,(4)} U^0 - b_0 U^0 + \eta_1, \\ \text{with } \|\eta_1\|_\infty \le C(\Delta t + h^4). \tag{A.1}$$

Subtracting the scheme (12) from the consistency estimate (A.1) and taking the discrete ℓ^2 inner product of the resulting equation with $\Delta t \bar{e}^1$ leads to

$$\|e^1_{[1]}\|_2^2 - \Delta t \langle \Delta_{h,(4)} e^1_{[1]}, e^1_{[1]} \rangle = \Delta t \langle e^1_{[1]}, \eta_1 \rangle, \tag{A.2}$$

where the fact $e^0 = 0$ has been used. Similar to the derivation of (37), we have

$$-\Delta t \langle \Delta_{h,(4)} e^1_{[1]}, e^1_{[1]} \rangle \ge \frac{45\Delta t}{48} \|\nabla_h e^1_{[1]}\|_2^2 + \frac{46\Delta t}{48} \cdot \frac{h^2}{12} (\|D_x^2 e^1_{[1]}\|_{2,n}^2 + \|D_y^2 e^1_{[1]}\|_{2,n}^2) \\ - \tilde{C}_1 \Delta t \|e^1_{[1]}\|^2 - \tilde{C}_1 \Delta t \cdot h^7.$$

By Cauchy's inequality, a combination of the above estimates, and (A.2), as well as the constraint $\Delta t \le \tilde{C} h$, indicates that

$$\|e^1_{[1]}\|_2^2 + \Delta t \big(\|\nabla_h e^1_{[1]}\|_2^2 + \frac{h^2}{12} (\|D_x^2 e^1_{[1]}\|_{2,n}^2 + \|D_y^2 e^1_{[1]}\|_{2,n}^2) \big) \le \tilde{C}_2 (\Delta t^2 + h^4)^2. \tag{A.3}$$

With the help of the ℓ^2 error estimate for (A.2), an application of the inverse inequality yields

$$\|e^1_{[1]}\|_\infty \le 2h^{-1} \|e^1_{[1]}\|_2 \le 2\tilde{C}_2^{\frac{1}{2}} h^{-1} (\Delta t^2 + h^4) \le 2\tilde{C}_2^{\frac{1}{2}} (\tilde{C}^2 h + h^3), \tag{A.4}$$

where the linear refinement $\Delta t \le \tilde{C} h$ has been used. We obtain $\|e^1_{[1]}\|_\infty < 1$ by setting $h \le \min\{1, (2\tilde{C}_2^{\frac{1}{2}} (\tilde{C}^2 + 1))^{-1}\}$. This in turn leads to

$$\|u^1_{[1]}\|_\infty \le \|U^1 - e^1_{[1]}\|_\infty \le \|U^1\|_\infty + \|e^1_{[1]}\|_\infty \le C^* + 1. \tag{A.5}$$

Next, we give an estimate of $e^1_{[2]} := U^1 - u^1_{[2]}$ updated by the corrector. The consistency analysis indicates that

$$\frac{U^1 - U^0}{\Delta t} - \Delta_{h,(4)} \frac{U^1 + U^0}{2} = \frac{1}{2} \big(f(U^0 + \theta(t_1) t_1^{-1} (U^1 - U^0), U^1) + f(U^0_\theta, U^0) \big) \\ - \boldsymbol{b} \cdot \nabla_{h,(4)} \frac{U^1 + U^0}{2} - b_0 \frac{U^1 + U^0}{2} + \eta_2, \\ \text{with } \|\eta_2\|_\infty \le C(\Delta t^2 + h^4). \tag{A.6}$$

Subtracting the scheme (13) with $l = 2$ from the consistency estimate (A.6), and taking the discrete ℓ^2 inner product of the resulting equation with $\Delta t \bar{e}^1$, leads to

$$2\|e^1_{[2]}\|_2^2 - \Delta t \langle \Delta_{h,(4)} e^1_{[2]}, e^1_{[2]} \rangle = \Delta t \langle \mathcal{NLE}^1_{[2]}, e^1_{[2]} \rangle - \Delta t \langle \boldsymbol{b} \cdot \nabla_{h,(4)} e^1_{[1]}, e^1_{[2]} \rangle \\ - \Delta t \langle b_0 e^1_{[1]}, e^1_{[2]} \rangle + 2\Delta t \langle \eta_2, e^1_{[2]} \rangle, \tag{A.7}$$

where $\mathcal{NLE}^1_{[2]} = f(u^0 + \theta(t_1) t_1^{-1} (u^1_{[1]} - u^0), u^1_{[1]}) - f(U^0 + \theta(t_1) t_1^{-1} (U^1 - U^0), U^1)$, and the relation $e^0 = 0$ has been used in the derivation. In a similar manner to the derivation in Section 2.2.3, we obtain

$$\|\mathcal{NLE}^1_{[2]}\|_2 \le 2 \max_{|\boldsymbol{\alpha}|=1, |v_1|, |v_2| \le 2(C^*+1)} |\partial^{\boldsymbol{\alpha}} f(v_1, v_2)| \cdot \|e^1_{[1]}\|_2 := \tilde{C}_3 \|e^1_{[1]}\|_2,$$

$$|\Delta t \langle \mathcal{NLE}^1_{[2]}, e^1_{[2]} \rangle| \le \frac{1}{8} \|e^1_{[2]}\|_2^2 + 2\tilde{C}_3 \Delta t^2 \|e^1_{[1]}\|_2^2,$$

$$-\Delta t \langle \Delta_{h,(4)} e^1_{[2]}, e^1_{[2]} \rangle \ge \frac{45\Delta t}{48} \|\nabla_h e^1_{[2]}\|_2^2 + \frac{46\Delta t}{48} \cdot \frac{h^2}{12} (\|D_x^2 e^1_{[2]}\|_{2,n}^2 + \|D_y^2 e^1_{[2]}\|_{2,n}^2) \\ - \frac{1}{8} \|e^1_{[2]}\|_2^2 - \tilde{C}_4 \Delta t \cdot h^7,$$

$$|\Delta t \langle \boldsymbol{b} \cdot \nabla_{h,(4)} e^1_{[1]}, e^1_{[2]} \rangle| \le \tilde{C}_5 \Delta t^2 h^4 (\|e^1_{[1]}\|_2^2 + \|\nabla_h e^1_{[1]}\|_2^2 + \|D_x^2 e^1_{[1]}\|_{2,n}^2 + \|D_y^2 e^1_{[1]}\|_{2,n}^2) \\ + \tilde{C}_5 \Delta t^2 \|\nabla_h e^1_{[1]}\|_2^2 + \frac{1}{8} \|e^1_{[2]}\|^2 + \tilde{C}_5 \Delta t^2 \cdot h^7,$$

$$|\Delta t \langle b_0 e^1_{[1]}, e^1_{[2]} \rangle| \le \frac{1}{8} \|e^1_{[2]}\|_2^2 + 2\Delta t^2 \|e^1_{[1]}\|_2^2,$$

$$2\Delta t \langle \eta_2, e^1_{[2]} \rangle \le \frac{1}{8} \|e^1_{[2]}\|_2^2 + 8\Delta t^2 \|\eta_2\|_2^2.$$

Using the above estimates and (A.3), we obtain from (A.7)

$$\|e^1_{[2]}\|_2^2 + \Delta t\big(\|\nabla_h e^1_{[2]}\|_2^2 + \frac{h^2}{12}(\|D_x^2 e^1_{[2]}\|_{2,n}^2 + \|D_y^2 e^1_{[2]}\|_{2,n}^2)\big) \le \tilde{C}_6(\Delta t^{2.5} + h^4)^2. \tag{A.8}$$

Furthermore, the estimate of $e^1 = e^1_{[3]}$ could be treated in the same way, i.e.,

$$\|e^1\|_2^2 + \Delta t\big(\|\nabla_h e^1\|_2^2 + \frac{h^2}{12}(\|D_x^2 e^1\|_{2,n}^2 + \|D_y^2 e^1\|_{2,n}^2)\big) \le \tilde{C}_7(\Delta t^3 + h^4)^2. \tag{A.9}$$

The estimates of $e^n, n = 2, 3$ could be analyzed in a similar way. In conclusion, we have, for $n = 1, 2, 3$,

$$\|e^n\|_2^2 + \Delta t\big(\|\nabla_h e^n\|_2^2 + \frac{h^2}{12}(\|D_x^2 e^n\|_{2,n}^2 + \|D_y^2 e^n\|_{2,n}^2)\big) \le C_0(\Delta t^3 + h^4)^2. \tag{A.10}$$

References

[1] Q. Du, L. Ju, X. Li, Z. Qiao, Stabilized linear semi-implicit schemes for the nonlocal Cahn-Hilliard equation, J. Comput. Phys. 363 (2018) 39–54.
[2] S. Shi, X. Du, W. Chen, A BDF-spectral method for a class of nonlocal partial differential equations with long time delay, SIAM J. Sci. Comput. 46 (2024) A3503–A3527.
[3] X. Shen, X. Yang, H. Zhang, S. Wang, A double reduction order nonlinear fourth-order difference method for the nonlinear nonlocal fourth-order PIDEs with a weakly singular kernel, Math. Meth. Appl. Sci. 49 (2025) 2885–2903.
[4] K. Liu, H. Zhang, X. Yang, An averaged $L1$ ADI compact difference scheme for the three-dimensional time-fractional mobile/immobile transport equation with weakly singular solutions, Comput. Math. Appl. 200 (2025) 102–116.
[5] S. Kochetov, G. Wollenberg, Stability of full-wave PEEC models: reason for instabilities and approach for correction, IEEE Trans. Electromagn. Compat. 47 (2005) 738–748.
[6] H. Wang, Y. Salmaniw, Open problems in PDE models for knowledge-based animal movement via nonlocal perception and cognitive mapping, J. Math. Biol. 86 (2023) 71.
[7] D.Green Jr., H.W. Stech, Diffusion and hereditary effects in a class of population models, in: Differential Equations and Applications in Ecology, Epidemics, and Population Problems, San Diego, Academic Press, 1981, pp. 19–28.
[8] V. Kolmanovskii, A. Myshkis, Introduction to the Theory and Applications of Functional Differential Equations, Springer Science & Business Media, 2013.
[9] J. Wu, Theory and Applications of Partial Functional Differential Equations, New York, Springer-Verlag, 1996.
[10] W. Wang, T. Rao, W. Shen, P. Zhong, A posteriori error analysis for Crank–Nicolson–Galerkin type methods for reaction-diffusion equations with delay, SIAM J. Sci. Comput. 40 (2018) A1095–A1120.
[11] C. Tang, C. Zhang, A fully discrete θ-method for solving semi-linear reaction-diffusion equations with time-variable delay, Math. Comput. Simulation 179 (2021) 48–56.
[12] C. Zhang, C. Tang, One-parameter orthogonal spline collocation methods for nonlinear two-dimensional Sobolev equations with time-variable delay, Commun. Nonlinear Sci. Numer. Simul. 108 (2022) 106233.
[13] X. Xu, Q. Huang, Discontinuous Galerkin time stepping for semilinear parabolic problems with time constant delay, J. Sci. Comput. 96 (2023) 57.
[14] H. Dai, Q. Huang, C. Wang, Exponential time differencing-Padé finite element method for nonlinear convection-diffusion-reaction equations with time constant delay, J. Comput. Math. 41 (2023) 370–394.
[15] Q. Huang, A. Ostermann, G. Zhong, Exponential Runge–Kutta methods of collocation type for parabolic equations with time-dependent delay, BIT Numer. Math. 66 (2026) 4.
[16] C. Huang, S. Vandewalle, An analysis of delay-dependent stability for ordinary and partial differential equations with fixed and distributed delays, SIAM J. Sci. Comput. 25 (2004) 1608–1632.
[17] C. Huang, S. Vandewalle, Unconditionally stable difference methods for delay partial differential equations, Numer. Math. 122 (2012) 579–601.
[18] J.R. Ockendon, A.B. Tayler, The dynamics of a current collection system for an electric locomotive, Proc. R. Soc. London A Math. Phys. Sci. 322 (1971) 447–468.
[19] J. Liang, J. Cao, Global exponential stability of reaction-diffusion recurrent neural networks with time-varying delays, Phys. Lett. A 314 (2003) 434–442.
[20] A.D. Polyanin, V.G. Sorokin, A.I. Zhurov, Delay Ordinary and Partial Differential Equations, CRC Press, Boca Raton, 2023.
[21] H. Brunner, Q. Huang, H. Xie, Discontinuous Galerkin methods for delay differential equations of pantograph type, SIAM J. Numer. Anal. 48 (2010) 1944–1967.
[22] Q. Huang, H. Xie, H. Brunner, Superconvergence of discontinuous Galerkin solutions for delay differential equations of pantograph type, SIAM J. Sci. Comput. 33 (2011) 2664–2684.
[23] Q. Huang, H. Xie, H. Brunner, The hp discontinuous Galerkin method for delay differential equations with nonlinear vanishing delay, SIAM J. Sci. Comput. 35 (2013) A1604–A1620.
[24] K. Ito, Z. Qiao, A high order compact MAC finite difference scheme for the Stokes equations: Augmented variable approach, J. Comput. Phys. 227 (2008) 8177–8190.
[25] W. E, J.-G. Liu, Essentially compact schemes for unsteady viscous incompressible flows, J. Comput. Phys. 126 (1996) 122–138.
[26] C. Wang, J.-G. Liu, H. Johnston, Analysis of a fourth order finite difference method for the incompressible Boussinesq equations, Numer. Math. 97 (2004) 555–594.
[27] J.-G. Liu, C. Wang, H. Johnston, A fourth order scheme for incompressible Boussinesq equations, J. Sci. Comput. 18 (2003) 253–285.
[28] J.-G. Liu, C. Wang, A fourth order numerical method for the primitive equations formulated in mean vorticity, Commun. Comput. Phys. 4 (2008) 26–55.
[29] R. Samelson, R. Temam, C. Wang, S. Wang, A fourth-order numerical method for the planetary geostrophic equations with inviscid geostrophic balance, Numer. Math. 107 (2007) 669–705.
[30] A. Fathy, C. Wang, J. Wilson, S. Yang, A fourth order difference scheme for the Maxwell equations on Yee grid, J. Hyperbolic Differ. Eq. 5 (2008) 613–642.
[31] K. Cheng, W. Feng, C. Wang, S.M. Wise, An energy stable fourth order finite difference scheme for the Cahn–Hilliard equation, J. Comput. Appl. Math. 362 (2019) 574–595.
[32] Z. Xia, C. Wang, L. Xu, Z. Zhang, High order accurate in time, fourth order finite difference schemes for the harmonic mapping flow, J. Comput. Appl. Math. 401 (2022) 113766.
[33] S. Gottlieb, C. Wang, Stability and convergence analysis of fully discrete Fourier collocation spectral method for 3-D viscous Burgers' equation, J. Sci. Comput. 53 (2012) 102–128.
[34] K. Cheng, C. Wang, Long time stability of high order multi-step numerical schemes for two-dimensional incompressible Navier–Stokes equations, SIAM J. Numer. Anal. 54 (2016) 3123–3144.
[35] K. Atkinson, W. Han, Theoretical Numerical Analysis: A Functional Analysis Framework, 39, Springer, third edition edition, 2005.
[36] E. Hairer, S.P. Nørsett, G. Wanner, Solving Ordinary Differential Equations I: Non-Stiff Problems, Springer, Berlin, Heidelberg,1993.
[37] X. Yang, Z. Zhang, Analysis of a new NFV scheme preserving DMP for two-dimensional sub-diffusion equation on distorted meshes, J. Sci. Comput. 99 (2024) 80.
[38] X. Yang, Z. Zhang, Superconvergence analysis of a robust orthogonal Gauss collocation method for 2D fourth-order subdiffusion equations, J. Sci. Comput. 100 (2024) 62.